Influence of ion sterics on diffusiophoresis and electrophoresis in concentrated electrolytes

Robert F. Stout and Aditya S. Khair*
Department of Chemical Engineering, Carnegie Mellon University, Pittsburgh, Pennsylvania 15213, USA
(Received 31 August 2016; published 6 January 2017)

We quantify the diffusiophoresis and electrophoresis of a uniformly charged, spherical colloid in a binary electrolyte using modified Poisson-Nernst-Planck equations that account for steric repulsion between finite sized ions. Specifically, we utilize the Bikerman (Bik) lattice gas model and the Carnahan-Starling (CS) and Boublik-Mansoori-Carnahan-Starling-Leland (BMCSL) equations of state for monodisperse and polydisperse, respectively, hard spheres. We compute the phoretic mobility for weak applied fields using an asymptotic approach for thin diffuse layers, where ion steric effects are expected to be most prevalent. The thin diffuse layer limit requires $\lambda_D/R \to 0$, where λ_D is the Debye screening length and R is the particle radius; this limit is readily attained for micron-sized colloids in concentrated electrolytic solutions. It is well known that the classic Poisson-Boltzmann (PB) model for pointlike, noninteracting ions leads to a prediction of a maximum in both the diffusiophoretic and electrophoretic mobilities with increasing particle zeta potential (at fixed λ_D/R). In contrast, we find that ion sterics essentially eliminate this maximum (for reasonably attainable zeta potentials) and increase the mobility relative to PB. Next, we consider the more experimentally relevant case of a particle with a constant surface charge density and vary the electrolyte concentration, neglecting charge regulation on surface active sites. Rather surprisingly, there is little difference between the predictions of the four models (PB, Bik, CS, and BMCSL) for electrophoretic mobility in concentrated solutions, at reasonable surface charge densities ($\sim$1–10 μC/cm^2). This is because as the concentration increases, the zeta potential is reduced (to below the thermal voltage for concentrations above about 1 M) and therefore the diffuse layer structure is largely unaffected by ion sterics. For gradients of symmetric electrolytes (equal diffusivities, charge, and size) diffusiophoresis is also essentially unaffected by ion sterics, with a mobility that approaches zero with increasing concentration, just as in electrophoresis. For gradients of asymmetric electrolytes, the difference in diffusivities of the cation and anions leads to an induced electric field that acts on the charged particle. Importantly, we show that ion sterics leads to an excess contribution to the induced electric field, which increases rapidly with concentration. This increase overwhelms the accompanying decrease in zeta potential. The result is the diffusiophoretic mobility increases with concentration, rather than approaching zero. Therefore, diffusiophoresis could be an appealing alternative transport mechanism to electrophoresis in concentrated electrolyte solutions.

DOI: 10.1103/PhysRevFluids.2.014201

I. INTRODUCTION

Electrophoresis is the motion of a charged colloidal particle under the influence of an electric field in an electrolyte solution [1]. Diffusiophoresis is the motion of a colloidal particle brought about by a concentration gradient of solute molecules that interact with the particle's surface via a long-ranged interaction potential [2,3]. For charged solute molecules (e.g., ions), the difference in diffusivities of the ions induces an electric field, which for a charged colloid produces electrophoretic motion. The excess of ions adjacent to the charged surface due to electrostatic attraction together with the

*akhair@andrew.cmu.edu

concentration gradient result in so-called chemiphoresis [2,4,5]. These two effects can support or counteract each other, depending on electrolyte species and particle zeta potential, ζ [2]. The sum of these effects is called diffusiophoresis. For nonelectrolyte solute molecules, diffusiophoresis is similar in nature [2–4], although generally weaker due to the absence of an induced electric field, making it difficult to observe in experiments [6]. In this case, the interaction between particle and solute is via van der Waals or other interaction potentials [3,7,8]. In this paper, we focus on diffusiophoresis in an electrolyte solution. Due to the similarities between diffusiophoresis and electrophoresis, we will keep the mathematical treatment general so it can be applied to both phenomena.

Diffusiophoresis was first described by Derjaguin *et al.* in 1947 [5], while electrophoresis has been known since (at least) the pioneering work of Smoluchowski in 1903 [9]. Electrophoresis is used extensively in microfluidics [10] and particle separation techniques [11,12]. Diffusiophoresis, on the other hand, has been slow to gain recognition of its impact on systems outside of laboratory settings. Nevertheless, recognition is increasing in applications of porous membrane filtration [13,14], flows in dead-end pores [15], focusing and spreading of particles [15,16], and detection and repair of cracks [17,18]. See [19] for a comprehensive review of the origins of diffusiophoresis. New microfluidic methods offer the ability to directly measure and observe diffusiophoresis [4], which has previously been difficult.

When subjected to an external electric field $\mathbf{E}^\infty$, a particle will migrate with an electrophoretic velocity $\mathbf{U} = M\mathbf{E}^\infty$ [1]. When instead exposed to a concentration gradient, the migration velocity is $\mathbf{U} = M\nabla \ln N^\infty$, where N^∞ is the number density of ions in the electroneutral bulk solution [2]. Note that in the previous two equations, the particle's phoretic mobility M is not the same, however, we retain a single symbol (M) for brevity. To predict the diffusiophoretic mobility, theoretical studies have almost exclusively been based on the Poisson-Boltzmann (PB) equation. Therein, the equilibrium relationship between the number density of ion species i, N_i and electrostatic potential ϕ is a Boltzmann distribution,

$$N_i = N_i^\infty \exp(-z_i \phi e / k_B T), \tag{1}$$

where N_i^∞ is the number density of ion species i in the electroneutral bulk solution, z_i is the ion charge number, and k_B, T, and e are the Boltzmann constant, temperature, and fundamental charge, respectively. This relationship establishes the structure of the "diffuse layer" of charge which screens the particle's surface charge. The diffuse layer has a characteristic width, $\lambda_D = \sqrt{\varepsilon k_B T / e^2 I}$, called the Debye length, where ε is the solution permittivity, and $I = \frac{1}{2}\sum_i z_i^2 N_i^\infty$ is the ionic strength. Prieve *et al.* [2] used the PB equation to predict the diffusiophoretic mobility of a spherical particle across a wide range of diffuse layer thicknesses (relative to the particle size), ζ potentials, and ionic species; for example, NaCl, NH_4F, and $KBrO_3$. They found that for some salts, the direction of particle migration could be reversed not only by changing the sign of the ζ potential but also by changing its magnitude.

The PB model assumes that the ions are point charges and have no interactions with each other, such as steric repulsion or electrostatic attraction or repulsion. However, this assumption can lead to unphysically large concentrations near highly charged surfaces or in concentrated electrolytes. For instance, consider a monovalent cation with hydrated volume v_+; the maximum density to which it can be packed is then $N_+^{\max} = 1/v_+$. Substituting this value into (1) and solving for the the electrostatic potential, we obtain $\zeta_c = (k_B T/e)\ln(v_+ N_+^\infty)$ as the critical ζ potential to achieve maximum packing [20]. Using Cs^+ as an example, the hydrated radius is 0.30 nm [21] and $v_+ = 0.216\ \text{nm}^3$. At a concentration of 1 M, $|\zeta_c| \sim 2(k_B T/e)$, about 50 mV, which is a realistic potential for colloids in physical systems. For this reason, the PB model is sometimes referred to as a dilute solution theory [22], since it is most valid in relatively dilute solutions, where ion interactions brought about by steric repulsion can be neglected.

However, there are systems of importance that contain concentrated electrolyte solutions, such as in enhanced oil recovery where brine solutions $O(1\ \text{M})$ are encountered [23,24]; mineral replacement reactions [19]; and energy generation from salinity gradients of sea water at river estuaries [25]. In order to describe the diffusiophoretic motion of colloidal particles in these systems, it is necessary

to incorporate ion-ion interactions into a description of the electrolyte. This is the central goal of the present paper. As a first step, we allow ions to interact sterically by accounting for their size in the governing equations for the structure of the diffuse layer and bulk solution.

One method of accounting for ion size is to establish a Stern layer adjacent to the particle surface [22]. The Stern layer is typically taken to be on the order of one ion radius in extent and acts as a capacitor in series with the diffuse layer. Although effective in eliminating the unphysical concentrations predicted by the PB equation, the Stern model only accounts for ion size at the solid surface and not throughout the diffuse layer or the electroneutral bulk solution. To do the latter, we instead modify the electrochemical potential μ_i of each ion species i to include an "excess" term,

$$\mu_i = \mu_i^{\mathrm{id}} + \mu_i^{\mathrm{ex}}, \tag{2}$$

where $\mu_i^{\mathrm{id}} = z_i e\phi + k_B T \ln N_i$ is the ideal contribution; and μ_i^{ex} is the "excess" electrochemical potential [22,26–28], which accounts for the entropic effect of ion size [28], allowing ions to interact with one another via steric repulsion.

The structure of the equilibrium diffuse layer is greatly affected by which model of μ_i^{ex} is used. For example, the simple Bikerman model [20,29] predicts that a maximum counterion concentration is achieved for large ζ potentials ($>\zeta_c$), while the Carnahan-Starling model [22,30] predicts lower concentrations at the surface with no maximum, but a more gradual decrease to the bulk concentration away from the surface. These models use the local density approximation (LDA), which defines the density of ions at a point based on only the information at that point [22,31]. This contrasts with methods used in density functional theory or molecular simulations (such as Monte Carlo or molecular dynamics) which use information throughout a specified volume to calculate an average density at each point [22,31,32]. While these nonlocal or weighted density approximations are capable of producing accurate descriptions of the diffuse layer at equilibrium, they are often computationally prohibitive to implement in the calculation of dynamic problems such as phoretic transport. This is because of the scale disparity between the size of the diffuse layer and of the particle: the former often being orders of magnitude smaller than the latter. Additionally, models based on the LDA have been shown to accurately capture integrated quantities such as capacitance of the diffuse layer [31,32], even though the detailed ion profiles differ from density functional theory and molecular simulations.

For electrophoresis, the assumption of pointlike ions leads to the prediction of a maximum in the mobility of a spherical particle with increasing ζ potential at $|\zeta| \sim O(k_B T/e)\ln(R/\lambda_D)$ [33–35], in the experimentally relevant thin diffuse layer limit ($\lambda_D/R \to 0$), where R is the particle radius. The maximum occurs because of surface conduction of the counterions in the diffuse layer, as described in Sec. IV(a) and [36]. Khair and Squires [26], employing Bikerman's model for excess electrochemical potential, showed that the maximum in electrophoretic mobility could be delayed to much larger ζ potentials—beyond the physical limits of most practical systems. Hence, ion sterics effectively eliminates the mobility maximum in electrophoresis. They argue that the surface conduction of counterions is reduced due to the constraint of a maximum packing density imposed by Bikerman's model. That is, there are simply fewer counterions near the surface relative to the PB model at the same ζ potential.

In this paper, we utilize three models of ion size in the calculation of the diffusiophoretic mobility of a uniformly charged spherical colloid in a weak electrolyte gradient for thin diffuse layers, $\lambda_D/R \to 0$. The three models are Bikerman [22,27–29], Carnahan-Starling [22,27,28], and Boublik-Mansoori-Carnahan-Starling-Leland [22,27,30,37]. Due to the mathematical similarity between diffusiophoresis and electrophoresis, we take a general approach that is applicable to both phoretic motions.

In Sec. II, we present the mathematics underlying the inclusion of ion size effects (steric repulsion). In Sec. III, we derive the general phoretic mobility equation. In Sec. IV, we present the results of mobility calculations based on a colloid with a varying ζ potential at a specified solution concentration (i.e., a single value of λ_D/R) which is a classic depiction of mobility variations in theoretical works [33]. In Sec. V, we present results for a colloid with a specified surface charge density with varying solution concentration, which is more relevant to how experiments are performed. Finally, in Sec. VI, we offer concluding remarks.

II. EQUILIBRIUM DIFFUSE LAYER AND MODIFIED ELECTROCHEMICAL POTENTIALS

Consider a spherical particle of radius R and uniform zeta potential ζ immersed in a binary electrolyte. Since we do not consider a Stern layer here, the ζ potential, which is formally the potential drop across the diffuse layer, can be equated with the potential at the particle's surface. The dimensionless number densities of cations and anions are n_+ and n_-, respectively, along with their respective charge numbers, z_+ and z_-. The charged surface attracts counterions and repels coions. This is balanced by Brownian diffusion, resulting in a diffuse layer of counter charge—a local counterion rich region near the surface. The structure of this equilibrium diffuse layer is described by Poisson's equation,

$$\epsilon^2 \nabla^2 \phi = -\sum_i z_i n_i, \tag{3a}$$

together with the condition of constant electrochemical potential at equilibrium,

$$\boldsymbol{\nabla} \mu_i = \mathbf{0}, \tag{3b}$$

where ϕ is the electrostatic potential and $\epsilon = \lambda_D/R$, where $\lambda_D = \sqrt{\varepsilon k_B T/e^2 I}$ is the Debye length, and the electrochemical potential is given by

$$\mu_i = z_i \phi + \ln N_i + \mu_i^{\text{ex}}. \tag{4}$$

In (3), and from here on, all quantities are dimensionless unless specified otherwise. The normalizations thus far are ϕ and $\zeta \sim k_B T/e, N_i \sim I, \mu_i \sim k_B T$, and $\boldsymbol{\nabla} \sim 1/R$, where k_B is Boltzmann's constant, T is temperature, e is the fundamental charge, ε is the solution permittivity, and $I = \frac{1}{2}\sum_i z_i^2 N_i^\infty$ is the ionic strength. The quantity $N_i = n_i I$ is the dimensional ion number density of species i. A superscript ∞ denotes reference to the electroneutral bulk solution.

Neglecting ion size by setting $\mu_i^{\text{ex}} = 0$, equation (3b) results in a Boltzmann relationship between electrostatic potential and ion density [1]. Substitution into (3a) then results in the Poisson-Boltzmann (PB) equation (1). Bikerman's model for ion size (which we abbreviate as "Bik") is one of the simplest modifications to the electrochemical potential that addresses the unphysical predictions of the PB equation. In the Bik model [22,29],

$$\mu_{i,\text{Bik}}^{\text{ex}} = -\ln(1-\Phi), \tag{5}$$

where $\Phi = \sum_i N_i v_i$ is the local volume fraction of ions and v_i is the dimensional hydrated volume of ion species i. The volume fraction varies from $0 \leqslant \Phi \leqslant 1$, where $\Phi = 1$ indicates that all of the solution at that point is occupied by ions. Importantly, Bik assumes that ions occupy sites on a regular lattice, so $v_i = a_i^3$, where a_i is the dimensional hydrated diameter of ion species i.

The attractiveness of using Bik is that one can derive a modified Poisson-Boltzmann equation (sometimes referred to as a Poisson-Bikerman equation [26]) by substituting (5) into (3) [22,26]. However, Bik can also underestimate excluded volume effects in the dilute limit, $\Phi \to 0$ [22,27]. To correct this, we could use $\mu_i^{\text{ex}} = -\ln(1-8\Phi)$ which accounts for the region of excluded volume around a sphere [27,28]. However, this now overestimates steric repulsion at larger Φ.

The second model we consider is Carnahan-Starling (abbreviated as "CS") which is derived from liquid state theory for monodisperse hard spheres [22,27,28,30]. As such, $v_i = \pi a_i^3/6$. In the CS model, the excess electrochemical potential is [22,27,28,30]

$$\mu_{i,\text{CS}}^{\text{ex}} = \frac{\Phi(8-9\Phi+3\Phi^2)}{(1-\Phi)^3}. \tag{6}$$

As Eqs. (5) and (6) indicate, μ_i^{ex} is equal for both species of ions for the Bik and CS models. This is because of the underlying assumption in Bik and CS that the ions are the same size and hence impose the same steric effects on one another. In this case, we assign each ion the average size of the pair, i.e., $a = (a_+ + a_-)/2$ is the ion size used in both the Bik and CS models for both cations and anions. This contrasts with the third model we consider, the Boublik-Mansoori-Carnahan-Starling-Leland

model (abbreviated as "BMCSL"), which is a generalization of CS for a mixture of hard spheres of differing size. As such, it explicitly accounts for different sized ions via an excess electrochemical potential [22,27,37,38],

$$\mu^{\mathrm{ex}}_{i,\mathrm{BMCSL}} = -\left[1 + 2\left(\frac{\xi_2 a_i}{\Phi}\right)^3 - 3\left(\frac{\xi_2 a_i}{\Phi}\right)^2\right]\ln(1-\Phi) + \frac{3\xi_2 a_i + 3\xi_1 a_i^2 + \xi_0 a_i^3}{1-\Phi} + \frac{3\xi_2 a_i^2}{(1-\Phi)^2}\left(\frac{\xi_2}{\Phi} + \xi_1 a_i\right) - \xi_2^3 a_i^3 \frac{\Phi^2 - 5\Phi + 2}{\Phi^2(1-\Phi)^3}, \tag{7}$$

where $\xi_k = \sum_j N_j v_j a_j^{k-3}$. By setting $a_+ = a_-$ and hence $v_+ = v_-$, the CS model (6) is recovered.

BMCSL is capable of producing qualitatively different results compared to Bik and CS. The primary difference being that for a multicomponent electrolyte, smaller counterions are predicted to be the dominant species near a highly charged surface, in preference to larger counterions [22,27]. This effect becomes greater as the surface charge is increased. However, since we consider only a binary electrolyte (and thus have only one counterion species) we do not observe this effect. Note, however, that for surfaces with charges that are equal in magnitude but opposite in sign, when the species which act as the counterion differ in size, the BMCSL model will predict different equilibrium profiles. In this case, the Bik, CS, and PB models will all predict the same profiles.

The assumption of Bik and CS that ions are of equal size contradicts them possibly having different diffusivities. Recall that the differences in diffusivities leads to an induced electric field that affects the diffusiophoretic mobility. Nevertheless, we ignore this contradiction and allow them to have unequal diffusivities. This is also why we consider the BMCSL model in order to more accurately portray differing ion size and as a check on the assumption of equal size.

In Fig. 1 we plot the equilibrium structure of the diffuse layer for a $c^\infty = 1$ M solution of KCl on a flat plate with $\zeta = 10$ and using $a_+ = 0.56$ nm and $a_- = 0.62$ nm [21] ($a = 0.59$ nm for Bik and CS). Whereas the PB model predicts an unbounded counterion density, the Bik model achieves

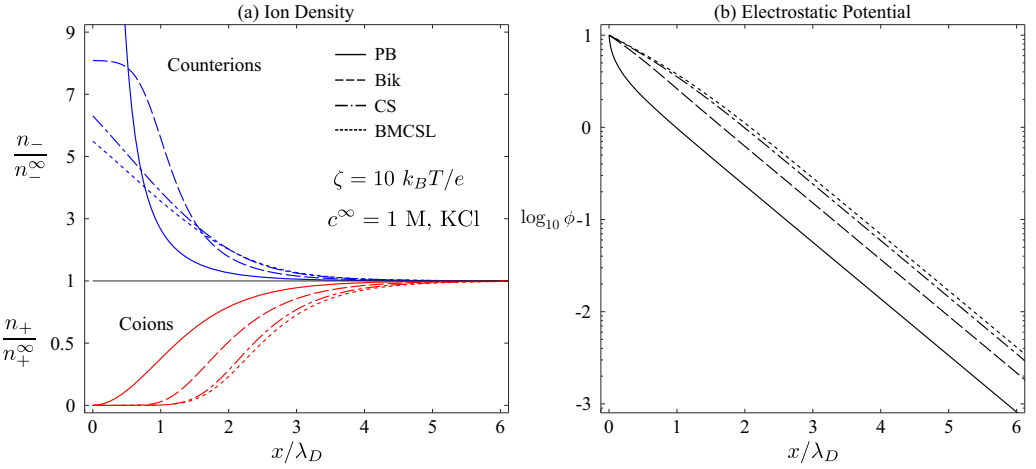

FIG. 1. Equilibrium ion density within the diffuse layer on a positively charged flat plate ($\zeta = 10$) for a 1 M solution of KCl. Shown are the ion densities from the Poisson-Boltzmann (PB), Bikerman (Bik), Carnahan-Starling (CS), and Boublik-Mansoori-Carnahan-Starling-Leland (BMCSL) models. The counterions increase in concentration near the surface while the coions are excluded. The Bik model achieves a saturation of counterions whereas the PB model predicts an unbounded concentration near the surface. The CS and BMCSL models predict lower concentrations of counterions but a more gradual decrease to the electroneutral bulk solution. (b) Equilibrium electrostatic potential within the diffuse layer. As the ion densities extend further away from the surface, so too do the electrostatic potentials.

a saturation of counterions (cnt), $n_{\text{cnt}}^{\max} = 2/N_{\text{cnt}}^{\infty} z_{\text{cnt}}(z_{\text{cnt}} - z_{\text{co}})\upsilon_{\text{cnt}}$, where z_{co} is the charge number of the coions.

From Fig. 1(a), both Bik and CS predict counterion densities that do not exponentially increase as one approaches the charged surface. The excess of counterions (relative to the bulk) also extends further away from the surface than for PB. The reason for this is the steric barrier to adding additional ions at any point is greater than with PB because of μ_i^{ex}. For instance, μ_i^{ex} increases more rapidly with Φ for CS than for Bik: for Bik, it is a slowly increasing logarithm, whereas for CS, it increases as $1/(1-\Phi)^3$, therefore the CS model favors lower ion densities than Bik. Further, in the dilute limit where $\Phi \to 0$, Bik is given by $\mu_{i,\text{Bik}}^{\text{ex}} \approx \Phi$ to first order whereas CS is given by $\mu_{i,\text{CS}}^{\text{ex}} \approx 8\Phi$, and we see the factor of 8 due to excluded volume that is not captured with Bik. The differences between the CS and BMCSL models demonstrates the effect of using different sized counterions (0.59 nm in CS versus the true 0.62 nm in BMCSL).

The equilibrium electrostatic potential, Fig. 1(b), shows that despite the high concentration and large ζ potential, the classic Debye-Hückel result is attained far from the surface. This is because beyond a few Debye lengths, the electrostatic potential is below both the critical voltage ζ_c and the thermal voltage. Here, electrostatic potential scales as $\phi \sim \exp(-x/\lambda_D)$ for all four models.

III. CALCULATING PHORETIC MOBILITY

A. Far field boundary conditions

Though conceptually different, electrophoresis (EP) and diffusiophoresis (DP) are mathematically similar. The essential difference is the boundary conditions in the electroneutral solution,

$$-\nabla\phi \to \mathbf{E}^{\infty}, \tag{8a}$$

$$n_i \to n_i^{\infty}, \tag{8b}$$

where $\mathbf{E}^{\infty}$ is the imposed uniform electric field in EP and a (possible) induced electric field in DP. In addition, the bulk concentration is constant in EP but varies according to the concentration gradient in DP. In the latter case, we use the bulk concentration and $\mathbf{E}^{\infty}$ that would exist at the center of the colloid if the particle were not present. As long as the concentration gradient is not strong (as we assume in the next section), the time dependence of the particle's position can be neglected, i.e., the diffusiophoretic problem is quasisteady.

To determine the induced electric field in a concentration gradient, consider that the ions will attempt to diffuse down the concentration gradient at different rates due to having unequal diffusivities. Countering this, and enforcing electroneutrality is an electric field (8a) that exactly balances the unequal diffusive fluxes and prevents a current from existing in the bulk solution. The net current is

$$\mathbf{J} = \sum_i z_i \mathbf{j}_i, \tag{9a}$$

where

$$\mathbf{j}_i = n_i(m\mathbf{v} - D_i\nabla\mu_i), \tag{9b}$$

is the flux of ion species i. In (9b), D_i is the diffusivity, $\mathbf{v}$ is the velocity of the fluid, and $m = \varepsilon(k_BT/e)^2/D\eta$, where η is the viscosity, and

$$D = \frac{(z_+ - z_-)D_+D_-}{z_+D_+ - z_-D_-} \tag{10}$$

is the effective salt diffusivity [39]. In the preceding, $\mathbf{j}_i \sim ID/R, |\mathbf{v}| \sim \varepsilon(k_BT/e)^2/R\eta$, and $D_i \sim D$. Note that Eq. (9b) is an approximation to the flux that is only strictly valid in dilute solutions, where

the diffusivity of ion, or solute, species can be taken as relative to the solvent only. A more detailed treatment of the ion flux would require using Stefan-Maxwell-like fluxes [40], which account for solute diffusion relative to other solute species as well as relative to the solvent. In addition, the motion of solute in the solution contributes to the average velocity of the solution, whereas (9b) assumes this is equal to the velocity of the solvent only. Nevertheless, Eq. (9b) along with excess electrochemical potentials serve as a reasonable starting point to consider concentrated solutions of ions.

Evaluating (9) in the bulk, where $n_i = n_i^\infty$, setting $\mathbf{J} = \mathbf{0}$, substituting (4), and rearranging yields the induced electric field,

$$\mathbf{E}^\infty = \beta^{\mathrm{id}} \boldsymbol{\nabla} \ln N_+^\infty + \frac{D_+ \boldsymbol{\nabla} \mu_+^{\mathrm{ex},\infty} - D_- \boldsymbol{\nabla} \mu_-^{\mathrm{ex},\infty}}{z_+ D_+ - z_- D_-}, \tag{11}$$

where $\beta^{\mathrm{id}} = (D_+ - D_-)/(z_+ D_+ - z_- D_-)$, and we have used the fact that $\mathbf{E}^\infty$ acts to enforce electroneutrality. The first term in (11) is equivalent to that derived by Chiang and Velegol [41] and Prieve *et al.* [2], the latter of whom considered the case of $z_+ = -z_- = 1$. The interesting part of (11) is the second term, which includes gradients of the excess electrochemical potential. These gradients can be understood as follows: within a concentration gradient of pointlike ions, there is a driving force for ion motion due to the ideal electrochemical potential. This generates a gradient in the electrostatic potential which drives ions based on their charge, and a gradient in the ion density which drives ions towards regions of lower concentration. However, in a gradient of ions with finite size, there is an additional ("excess") driving force due to the steric repulsion between the ions. This additional contribution manifests as a gradient in the excess electrochemical potential and drives ions to move towards regions of lower steric repulsion. It will be shown that this additional contribution to $\mathbf{E}^\infty$ is significant for diffusiophoresis in concentrated electrolytes.

To make progress with the gradients in the second term of (11), we observe that the only variable all three models for μ_i^{ex} (5)–(7) depend on is the volume fraction Φ, hence $\boldsymbol{\nabla} \mu_i^{\mathrm{ex},\infty} = (d\mu_i^{\mathrm{ex},\infty}/d\Phi^\infty) \boldsymbol{\nabla} \Phi^\infty$. Further, we define

$$H_i^\infty = \frac{d\mu_i^{\mathrm{ex},\infty}}{d\Phi^\infty} \Phi^\infty, \tag{12}$$

such that $\boldsymbol{\nabla} \mu_i^{\mathrm{ex},\infty} = H_i^\infty \boldsymbol{\nabla} \ln N_+^\infty$, where we have made use of the fact that for a binary electrolyte, $\boldsymbol{\nabla} \ln \Phi^\infty = \boldsymbol{\nabla} \ln N_+^\infty = \boldsymbol{\nabla} \ln N_-^\infty$. Substituting the above into (11) gives

$$\mathbf{E}^\infty = (\beta^{\mathrm{id}} + \beta^{\mathrm{ex}}) \boldsymbol{\nabla} \ln N_+^\infty, \tag{13a}$$

where

$$\beta^{\mathrm{ex}} = \frac{D_+ H_+^\infty - D_- H_-^\infty}{z_+ D_+ - z_- D_-}, \tag{13b}$$

acts as an "excess" contribution to the induced electric field that, like β^{id}, is a constant parameter of a given electrolyte pair but depends on the volume fraction through (12). This additional term serves to enhance the induced electric field. To see this, recall that Bik and CS assign each species the same excess potential, hence $H_+^\infty = H_-^\infty = H^\infty$. In this case, (13) reduces to

$$\mathbf{E}^\infty = \beta^{\mathrm{id}} (1 + H^\infty) \boldsymbol{\nabla} \ln N_+^\infty. \tag{14}$$

Further, since $0 \leqslant \Phi^\infty \leqslant 1$, it can be shown that $(d\mu_i^{\mathrm{ex},\infty}/d\Phi^\infty) > 0$, which means that an increase in ion volume fraction—whether by additional ions or increased ion size—makes further increases less favorable and leads to $H^\infty > 0$. Therefore (14) represents an increase to the induced electric field over that predicted for an ideal solution, $H_i^\infty = 0$.

Substituting (13) [or (14)] into (8), we can write a general form for the far field boundary conditions:

$$-\nabla\phi \to \theta\mathbf{V}, \tag{15a}$$

$$n_i \to n_i^{\infty}, \tag{15b}$$

where

$$\theta = \begin{cases} 1, & \text{for EP} \\ \beta^{\text{id}} + \frac{D_+H_+^{\infty} - D_-H_-^{\infty}}{z_+D_+ - z_-D_-}, & \text{for DP} \end{cases} \tag{15c}$$

is a generalized scale for the induced or applied electric field, and

$$\mathbf{V} = \begin{cases} \mathbf{E}^{\infty}, & \text{for EP} \\ \nabla \ln N_+^{\infty}, & \text{for DP,} \end{cases} \tag{16}$$

such that $\mathbf{E}^{\infty} = \theta\mathbf{V}$. Note that $\nabla \ln N_+^{\infty}$ in (16) could be replaced by any equivalent measure of concentration in the bulk (e.g., $I, N_-^{\infty}, N_+^{\infty}$) since for a binary electrolyte $\nabla \ln N_+^{\infty} = \nabla \ln N_-^{\infty} = \nabla \ln I = \nabla \ln c^{\infty} = \nabla \ln \Phi^{\infty}$.

Boundary conditions (15) can be combined with (4) to form a far field boundary condition on the electrochemical potential,

$$\nabla\mu_i \to G_i\mathbf{V}, \tag{17a}$$

where

$$G_i = \begin{cases} -z_i\theta, & \text{for EP} \\ -z_i\theta + 1 + H_i^{\infty}, & \text{for DP,} \end{cases} \tag{17b}$$

which allows us to collect all of the mathematical differences between EP and DP into a single quantity, G_i. Now the derivation for phoretic mobility can be performed generally by using (15) and (17), as we do in the next subsection.

B. Phoretic mobility: Thin diffuse layer analysis

To drive the spherical colloid into motion, a uniform gradient of either electrostatic potential or electrolyte concentration is imposed. We denote the resulting "driving" vector generally as $\mathbf{V}$ and give its two forms in (16). Importantly, we assume that $|\mathbf{V}| \ll 1$; more specifically,

$$|\mathbf{E}^{\infty}| \ll 1, \quad \text{for EP,} \tag{18a}$$

$$|\nabla \ln N_+^{\infty}| \ll 1, \quad \text{for DP,} \tag{18b}$$

where (18a) arises from the dimensional comparison $|\mathbf{E}^{\infty}| \ll k_BT/eR$, and (18b) from the dimensional comparison $|\nabla N_+^{\infty}| \ll N_+^{\infty}/R$, which state that the applied electrostatic potential and electrolyte concentration, respectively, do not vary appreciably on the scale of the particle. This condition is readily met for concentration gradients when the concentration is large. For example, for a 1 M concentration and a particle with radius 200 nm, according to the dimensional comparison above, the concentration gradient would need to be less than 50 000 M/cm.

These imposed gradients cause the spherical particle to move at a velocity $\mathbf{U} = M\mathbf{V}$, where M is the phoretic mobility of the particle, $|\mathbf{U}| \sim \varepsilon(k_BT/e)^2/R\eta$, and $M \sim \varepsilon(k_BT/e)/\eta$ for EP and $M \sim \varepsilon(k_BT/e)^2/\eta$ for DP. Despite the seeming simplicity of this equation, considerable effort has been made to calculate the value of M under a variety of conditions for both EP and DP [2,3,9,26,33,35,42]. Often, the Poisson equation (3a) is used together with

$$\frac{\partial n_i}{\partial t} = -\epsilon\nabla\cdot\mathbf{j}_i, \tag{19}$$

to describe the electrolyte dynamics. Equation (19) is the Nernst-Planck equation where t is time scaled by the RC time, $\lambda_D R/D$. Together, (3a) and (19) are the Poisson-Nernst-Planck (PNP) equations. We can simplify (19) by making the assumption that the problem is independent of time since (18b) implies that as the particle moves, the concentration evolves quasisteadily [2]. Thus,

$$\boldsymbol{\nabla}\cdot\mathbf{j}_i = 0. \tag{20}$$

To solve for the fluid velocity, the Stokes equations are used,

$$\nabla^2\mathbf{v} - \boldsymbol{\nabla} P = \sum_i n_i \boldsymbol{\nabla}\mu_i/\epsilon^2, \tag{21a}$$

$$\boldsymbol{\nabla}\cdot\mathbf{v} = 0. \tag{21b}$$

Equation (21a) is conservation of momentum with an electrochemical body force term to account for the ions. Equation (21b) is conservation of mass.

In a reference frame fixed at the particle center (such that $\mathbf{v} \to -\mathbf{U}$ far from the colloid), these equations are supplemented with boundary conditions at the particle surface,

$$\phi = \zeta, \tag{22a}$$

$$\mathbf{v} = \mathbf{0}, \tag{22b}$$

$$\hat{\mathbf{n}}\cdot\boldsymbol{\nabla}\mu_i = 0, \tag{22c}$$

where $\hat{\mathbf{n}}$ is the unit normal to the surface. Equations (22b) and (22c) specify no-slip and no flux of ions through the surface, respectively. Of course, we also utilize a boundary condition far from the surface, (15) and (17), developed in the previous subsection. In Sec. V, we replace (22a) with a constant surface charge density boundary condition.

Our derivation of the mobility equation follows closely that of O'Brien and White [33] and Khair and Squires [26]. To proceed, we express the unknowns in terms of a perturbation about their equilibrium values,

$$\phi = \phi^0 + \phi^1|\mathbf{V}|, \tag{23a}$$

$$n_i = n_i^0 + n_i^1|\mathbf{V}|, \tag{23b}$$

$$\mu_i = \mu_i^0 + \mu_i^1|\mathbf{V}|, \tag{23c}$$

$$\mathbf{v} = \mathbf{v}^0 + \mathbf{v}^1|\mathbf{V}|, \tag{23d}$$

where a superscript 0 denotes the equilibrium value and a superscript 1 denotes the perturbation. Substituting (23) into the governing equations (3), (20), and (21); the boundary conditions (15), (17), and (22); and neglecting all terms $O(|\mathbf{V}|^2)$ and higher, we obtain a set of linear differential equations governing the equilibrium and $O(|\mathbf{V}|)$ problems. Since the equilibrium problem has no imposed field, $\mathbf{v}^0 = \mathbf{0}$ and we are left with only Poisson's equation (3a) and constancy of electrochemical potential (3b) describing the equilibrium problem. The perturbed, $O(|\mathbf{V}|)$, equations are

$$\epsilon^2\nabla^2\phi^1 = -\sum_i z_i n_i^1, \tag{24a}$$

$$m\boldsymbol{\nabla}n_i^0\cdot\mathbf{v}^1 = D_i\boldsymbol{\nabla}\cdot\left(n_i^0\boldsymbol{\nabla}\mu_i^1\right), \tag{24b}$$

$$\epsilon^2\nabla^2(\boldsymbol{\nabla}\times\mathbf{v}^1) = \sum_i\left(\boldsymbol{\nabla}n_i^0\times\boldsymbol{\nabla}\mu_i^1\right), \tag{24c}$$

where (24c) results from taking the curl of the perturbed (21a) to eliminate pressure.

By considering the limit of thin diffuse layers, $\epsilon \to 0$, we can considerably simplify these equations. In this limit, the majority of the electrolyte is electroneutral except for a locally planar region near the surface of the colloid. For a more formal asymptotic analysis of this limit see [35,43].

A key outcome is that, to leading order in ϵ, the perturbed electrochemical potential is constant across the diffuse layer, $\partial\mu_i^1/\partial y = 0$, where $y = (r-1)/\epsilon$ is a local coordinate perpendicular to the particle surface. Upon rescaling (24) with y, we find that the perpendicular fluid flow is negligible compared to the tangential component in the diffuse layer; the latter is given by [26]

$$\mathbf{v}^1 = -\sum_i \nabla_s \mu_i^1 \int_0^y \int_{y'}^\infty \left(n_i^0 - n_i^\infty\right) dy'' dy', \tag{25}$$

where $\nabla_s = (\mathbf{I} - \hat{\mathbf{n}}\hat{\mathbf{n}}) \cdot \nabla$ is the surface gradient operator and the sum is over both ion species, $i = +$ and $i = -$. The quantity $(n_i^0 - n_i^\infty)$ represents the concentration of ions within the diffuse layer relative to the electroneutral solution. To calculate the mobility we require the "slip" velocity which is obtained from the limit $y \to \infty$ of (25), that is, the velocity just outside the diffuse layer. The slip velocity is thus [26]

$$\mathbf{v}_s^1 = -\sum_i \nabla_s \mu_i^1 \int_0^\infty y\left(n_i^0 - n_i^\infty\right) dy. \tag{26}$$

To determine the perturbed electrochemical potentials, we require that at the "interface" between the diffuse layer and bulk solution ($y \to \infty$ or $r \to 1$, with ϵ fixed), all quantities (n_i, μ_i, etc.), are continuous. This means that since n_i^0 is constant in the bulk, we have from Eq. (24b) that $\nabla^2 \mu_i^1 = 0$ throughout the bulk. Solving this subject to boundary condition (17) we obtain

$$\mu_i^1 = (G_i + C_i r^{-3}) \mathbf{V} \cdot \mathbf{r}, \tag{27}$$

where $\mathbf{r}$ is the position from the center of the sphere, and C_i are integration constants to be determined below.

The mobility is then calculated by averaging $\mathbf{v}_s^1$ over the surface of the sphere [44],

$$M\mathbf{V} = -\frac{1}{4\pi} \int_S \mathbf{v}_s^1 dS. \tag{28}$$

The mobility is thereby

$$M = \frac{2}{3} \sum_i \left[(G_i + C_i) \int_0^\infty y\left(n_i^0 - n_i^\infty\right) dy \right]. \tag{29}$$

From (29), we see that it is the deviation of ion density relative to its value in the bulk, $n_i^0 - n_i^\infty$, that arises in the mobility equation, as opposed to the actual value of ion density, n_i^0, at a location y.

The remaining constants, C_i, are computed by establishing effective boundary conditions for μ_i^1 between the diffuse layer and the bulk. This is done by balancing the normal flux of ions between the diffuse layer and the bulk with the variation in the tangential flux. Following [26], these boundary conditions are

$$\frac{\partial \mu_i^1}{\partial r} = \left(f_i \nabla_s^2 \mu_i^1 + g_i \nabla_s^2 \mu_j^1\right), \quad \text{at } r = 1, \tag{30}$$

where $i \neq j$ and

$$f_i = -\epsilon D_i \int_0^\infty \left(n_i^0 - n_i^\infty\right) dy - \epsilon m \int_0^\infty \left(n_i^0 - n_i^\infty\right) I_i dy, \tag{31a}$$

$$g_i = -\epsilon m \int_0^\infty \left(n_i^0 - n_i^\infty\right) I_j dy, \tag{31b}$$

where $I_i = \int_0^y \int_{y'}^\infty (n_i^0 - n_i^\infty) dy'' dy'$. The C_i are then

$$C_i = \frac{G_i[2g_i g_j - (2f_i + 1)(f_j - 1)] + 3G_j g_i}{2(f_i - 1)(f_j - 1) - 2g_i g_j}. \tag{32}$$

Substituting (32) into (29) yields an equation which explicitly shows the dependence of the mobility on G_i, that is, on whether EP or DP is considered,

$$M = \sum_i \left[\left(\frac{G_i(1-f_j) + g_i G_j}{(f_i-1)(f_j-1) - g_i g_j} \right) \int_0^\infty y\left(n_i^0 - n_i^\infty\right) dy \right], \tag{33}$$

where again $i \neq j$.

Equations (29) and (33) are general expressions of both electrophoretic and diffusiophoretic mobility for a spherical colloid in a binary electrolyte, where z_+ and z_- are not necessarily equal. Ion steric effects (steric repulsion) are contained within the equilibrium ion densities n_i^0 and the phoresis dependent far field electrochemical potential gradient G_i (17b).

IV. PHORETIC MOBILITY: FOR VARYING ζ POTENTIAL AT FIXED CONCENTRATION

In our calculations that follow, all hydrated ion size data are taken from Ohtaki and Radai [21]. The reported size of hydrated ions varies depending on the experimental methods and theories used to determine it. For more information on this, as well as extensive tables of ion size data, see [21]. All diffusivity data are taken from Flury and Gimmi [45] (Table 6.2-1), which is calculated from conductance in the limit of low concentration. Their Table 6.2-2 shows that the concentration dependence of salt diffusivity is weak up to a concentration of 1 M. Beyond that, the diffusivity is expected to decrease approximately as $D_i = D_{i,o}(1-\Phi_i)$, where $D_{i,o}$ is the diffusivity in a dilute solution [46]. Incorporating a concentration dependent diffusivity would require including D_i in the integral of Eqs. (31). However, since $\epsilon \ll 1$ at large concentrations, this change has little impact on the mobility. The induced electric field would be affected via the dependence of β^{id} and β^{ex} on ion diffusivity for the BMCSL model only, since the other models assume each ion species has the same size (and hence the same volume fraction). Although β^{id} could be significantly reduced, e.g., for NaCl from a value of -0.2074 in a dilute solution to -0.0719 at 5 M, β^{ex} will continue to increase rapidly with concentration. This is because, as we give in the Appendix, H_i^∞ diverges more rapidly than the diffusivity vanishes as $\Phi^\infty \to 1$. Hence the qualitative results presented in this paper are not affected by the use of a dilute solution value of the diffusivity.

To characterize the effect of the surface conduction of ions within the diffuse layer on the mobility, we utilize the dimensionless Dukhin number, $\mathrm{Du} = \sigma_s/\sigma_b$, which is a measure of the surface conductivity σ_s relative to the conductivity in the bulk σ_b. The bulk conductivity is just the electrical conductivity, $\sigma_b = \sum_i z_i^2 D_i n_i^\infty$, in the electroneutral bulk solution [36]. Note that although there is no current in the bulk solution for DP, there is still a conductivity given by σ_b. Defining the surface conductivity by the surface current, $\mathbf{J}_s = \sigma_s \mathbf{V}$, and the driving vector $\mathbf{V}$, we can derive a generalized Dukhin number that is valid for both EP and DP.

Substituting (9b) into (9a), the total current is given by $\mathbf{J} = \rho m \mathbf{v} - \sum_i z_i D_i n_i \nabla \mu_i$, where $\rho = \sum_i z_i n_i$ is the charge density. Applying this to the bulk solution, where $n_i = n_i^\infty$ and $\rho = 0$, and substituting (4) for μ_i, we obtain $\mathbf{J}_b = \sum_i z_i^2 D_i n_i^\infty \mathbf{E}^\infty - \sum_i z_i D_i n_i^\infty G_{i,\mathrm{DP}} \mathbf{V}$ for the current in the bulk solution, where $G_{i,\mathrm{DP}} = 1 + H_i^\infty$ is the contribution to $\nabla \mu_i^\infty$ due to a concentration gradient. The surface current is then the current in excess of $\mathbf{J}_b$, integrated over the diffuse layer, $\mathbf{J}_s = \epsilon \int_0^\infty (\mathbf{J} - \mathbf{J}_b) \mathrm{d}y$. Substituting (25), (17), and using the fact that $\partial \mu_i^1 / \partial y = 0$ within the diffuse layer, we obtain

$$\mathbf{J}_s = \epsilon \int_0^\infty \left[\sum_i z_i^2 D_i \left(n_i^0 - n_i^\infty\right) \theta - \rho^0 m \sum_i G_i I_i - \sum_i z_i D_i \left(n_i^0 - n_i^\infty\right) G_{i,\mathrm{DP}} \right] dy \mathbf{V}, \tag{34}$$

where we have also made use of the fact that $\mathbf{E}^\infty = \theta \mathbf{V}$. The first term in (34) is due to the electromigration of ions with the electric field (induced or applied). The second term is due to

convection of ions with the electro- and chemiosmotic fluid flow. The third term represents the contribution from ions diffusing down the concentration gradient.

The generalized Dukhin number is therefore given by

$$\mathrm{Du} = \frac{\epsilon}{\sum_i \left(z_i^2 D_i n_i^\infty\right)} \int_0^\infty \left[\sum_i z_i^2 D_i \left(n_i^0 - n_i^\infty\right)\theta - \rho^0 m \sum_i G_i I_i - \sum_i z_i D_i \left(n_i^0 - n_i^\infty\right) G_{i,\mathrm{DP}} \right] dy. \tag{35}$$

Note that for EP, $G_{i,\mathrm{DP}} = 0$ since there is no applied concentration gradient; in this case, the usual definition of the Dukhin number is recovered [26,36,47].

A. Electrophoresis

Figure 2(a) shows the electrophoretic mobility for a 1 M KCl solution with $\epsilon = 0.01$ for PB, Bik, CS, and BMCSL over the range $\zeta = -10$ to 10. First note that the negative ζ potentials have negative mobilities whereas the positive potentials give positive mobilities, i.e., negatively (positively) charged particles move against (with) the applied field. The PB model predicts a maximum in the mobility at $\zeta \sim \pm 6.5$, whereas Bik, CS, and BMCSL predict a continuously increasing mobility over the range of ζ shown. The maximum in PB is due to the increasing importance of surface conduction with exponentially increasing counterion concentration in the diffuse layer [35]. This is reflected

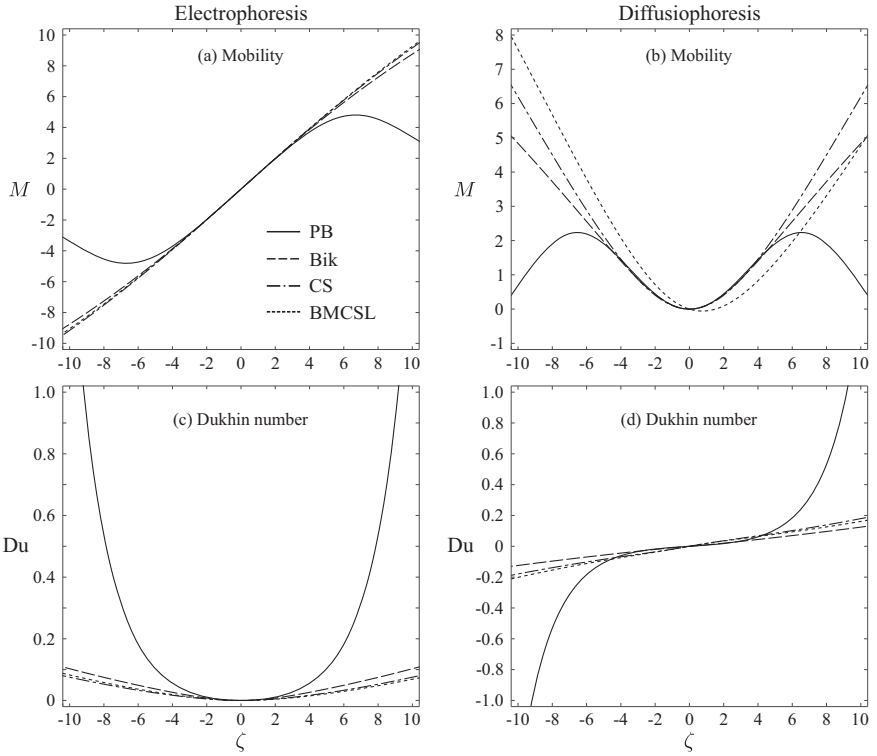

FIG. 2. Phoretic mobility for a 1 M solution of KCl with $\epsilon = 0.01$ for all four models of ion size: Electrophoretic mobility (a) and corresponding Dukhin number (c) vs ζ potential; diffusiophoretic mobility (b) and corresponding Dukhin number (d) vs ζ potential. Diffusiophoretic plots (b) and (d) assume equal diffusivities for the cation and anion, $D_+ = D_-$, leading to $\beta^{\mathrm{id}} = 0$.

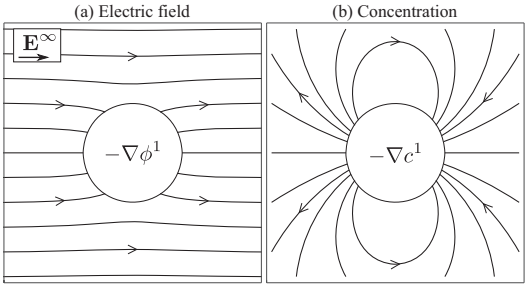

FIG. 3. Streamlines of the electric field (a) and concentration flux (b) for electrophoresis using the PB model for $\zeta \to +\infty$ and ϵ fixed, such that $\mathrm{Du} \to +\infty$.

in Fig. 2(c), which is a plot of Du versus ζ. As ζ increases (in magnitude), the surface conduction increases rapidly until it offsets further increases in mobility.

To see how surface conduction affects the mobility (in the case of PB) it is instructive to consider the (academic) limit $\zeta \to \infty$ with ϵ fixed (i.e., $\mathrm{Du} \to \infty$). Here, the constants C_i in (27) adopt values for a conductor of counterions, $C_{\mathrm{cnt}} = -G_{\mathrm{cnt}}$, and an insulator of coions, $C_{\mathrm{co}} = G_{\mathrm{co}}/2$. This ensures that a maximal flux of counter charge can be exchanged between the bulk solution and diffuse layer. Then using these values for C_i together with (4) we can derive equations for the perturbed electric potential and ion density in the bulk. The derivation is given in the Appendix along with the full expressions for both EP and DP; here, we give simplified forms relevant to a symmetric, monovalent electrolyte. For electrophoresis these equations are

$$\phi^1 = -\left(1 - \frac{1}{4r^3}\right)\mathbf{E}^\infty \cdot \mathbf{r}, \tag{36a}$$

$$c^1 = n_+^1 + n_-^1 = -\frac{3\mathrm{sgn}(\zeta)}{2r^3}\mathbf{E}^\infty \cdot \mathbf{r}, \tag{36b}$$

where $\mathrm{sgn}(\zeta)$ is the sign of ζ.

These equations are identical to those given by Khair and Squires [36]. Figure 3 is streamlines of the electric field, $-\boldsymbol{\nabla}\phi^1$, and concentration gradient, $-\boldsymbol{\nabla}c^1$ showing the direction of neutral salt motion, for a positively charged particle. These figures again are identical to those produced by Khair and Squires [36] but are reproduced here to contrast with the forthcoming predictions for DP.

Figure 3(a) shows that the applied electric field is uniform far from the sphere but varies across the surface, where the "surface" is the interface between the thin diffuse layer and the bulk solution. In particular, the tangential component, which is zero at the poles and maximum at the equator, drives a tangentially varying surface flux of counterions (surface conduction). This necessitates that the negative counterions be exchanged between the diffuse layer and bulk solution. This exchange occurs along the electric field lines and counterions exit the diffuse layer in the upstream and enter in the downstream, relative to the applied electric field, $\mathbf{E}^\infty$. Of course, the positive coions also move along these bulk field lines but are excluded from the diffuse layer. The result is a concentration polarization in the bulk with a greater concentration in the upstream region and a chemiosmotic flow due to gradients in neutral salt [Fig. 3(b)], from upstream to downstream, which counteracts the electro-osmotic flow and reduces the mobility.

Accounting for steric repulsion between ions eliminates the exponential increase of counterions in the diffuse layer, which means a reduced surface conduction of counterions; consequently, the mobility continues to increase. In fact, for $\epsilon = 0$ with ζ fixed and finite, surface conduction becomes negligible, and all four models approach limiting lines. The slopes of these lines are dependent on the model since the equilibrium diffuse layers have differing structures. In the case of the PB model,

the classic Helmholtz-Smoluchowski mobility, $M = \zeta$, is recovered. In general, for $\epsilon \equiv 0$ with ζ fixed, $C_i = G_i/2$ and

$$M = \sum_i \left[G_i \int_0^\infty y\left(n_i^0 - n_i^\infty\right) dy \right], \tag{37}$$

which is valid for both EP and DP but resists analytic treatment for $\mu_i^{\text{ex}} \neq 0$.

Finally, all four models agree in a range of ζ between about -3 and 3, suggesting that for potentials below about ± 75 mV, steric repulsion between ion does not significantly affect electrophoretic mobility—even in rather concentrated solutions.

B. Diffusiophoresis

1. *Symmetric electrolytes ($D_+ = D_-$)*

Although similar mathematically to electrophoresis, the induced electric field (13) brought about by diffusivity differences and steric repulsion between ions adds a unique feature to diffusiophoresis. As such, we will first consider an idealized example of KCl in which we assume the diffusivities are equal and hence $\beta^{\text{id}} = 0$. Note that the actual value for KCl is $\beta^{\text{id}} = -0.0188$. A consequence of this assumption is that the induced electric field is nonexistent for PB, Bik, and CS and the situation resembles that of DP in nonelectrolytes. For BMCSL, since $H_+^\infty \neq H_-^\infty$, then $\beta^{\text{ex}} \neq 0$ and an induced electric field exists due solely to steric repulsion between ions as a result of ion size differences.

Figure 2(c) shows the diffusiophoretic mobility for a 1-M KCl solution with $\epsilon = 0.01$ for PB, Bik, CS, and BMCSL over the range $\zeta = -10$ to 10. Unlike in EP, the PB, Bik, and CS models all predict a symmetric mobility about $\zeta = 0$. This is expected since, in the absence of an induced electric field, the particle will prefer to move towards regions of higher ion concentration, i.e., in the direction of the concentration gradient. Therefore, the mobility is symmetric due to neglecting diffusivity differences and assuming both ion species are the same size (or zero size in PB).

This behavior contrasts with what the BMCSL model predicts, which allows for different sized ions. The asymmetry in BMCSL is due primarily to the induced electric field arising from ion size (β^{ex}) as explained above. Another factor is that when $\zeta < 0$, the smaller ion, K^+, is the counterion which is able to more tightly pack in the diffuse layer than Cl^- when $\zeta > 0$ and it is the counterion. This results in differing equilibrium diffuse layer structures on either side of $\zeta = 0$ and hence an asymmetric mobility. This second factor is much less significant than the induced electric field. In fact, although we do not show this result, by setting $\beta^{\text{ex}} = 0$ (neglecting the induced electric field completely, i.e., $\theta = 0$) the BMCSL model gives mobilities which are much closer to the CS model results. This is despite predicting quantitatively different diffuse layer structures (see Fig. 1), which demonstrates how integrated quantities such as mobility and diffuse layer capacitance do not have a strong dependence on the structure of the equilibrium diffuse layer, for differing models that account for ion size.

Figure 2(d) shows the Dukhin number for diffusiophoresis. As with EP, the PB model predicts a large increase in surface conduction along with a corresponding maximum in mobility. Although Du is always positive for electrophoresis, our generalized Du can take on negative values for DP. However, it is the magnitude of Du which is important. The PB model gives a much lager |Du| than Bik, CS, or BMCSL, indicating significantly greater surface conduction in DP, just as in EP.

The negative values of Du occur because the convective, $-\epsilon \int_0^\infty \rho^0 m \sum_i G_i I_i dy \mathbf{V}$, and concentration gradient, $-\epsilon \int_0^\infty \sum_i z_i D_i (n_i^0 - n_i^\infty) G_{i,\text{DP}} dy \mathbf{V}$, contributions to the surface current can be either positive or negative. Since the convective flux is in the opposite direction as particle migration, if positively and negatively charged particles migrate in the same direction (as they do in DP for reasonable ζ potentials), then the convective current will be in opposite directions due to having oppositely charged diffuse layers. Similarly, the flux due to the concentration gradient is always in the same direction and oppositely charged diffuse layers will result in positive or negative

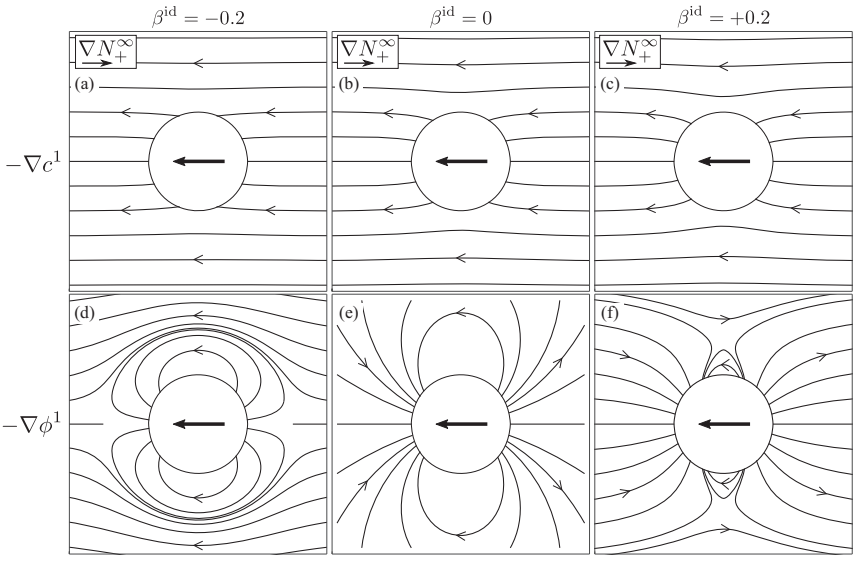

FIG. 4. Streamlines of concentration flux (a)–(c) and electric field (d)–(f) for diffusiophoresis using the PB model for three representative values of β^{id} as $\zeta \to +\infty$ and ϵ fixed such that $|\mathrm{Du}| \to \infty$. The varying tangential component of the concentration flux gives rise to a surface conduction induced local electric field for all three values of β^{id}, which provides field lines along which charge can be exchanged between the diffuse layer and the electroneutral bulk. Far from the particle, away from the local electric field, the induced electric field $\mathbf{E}^\infty$ is recovered for $\beta^{\mathrm{id}} \neq 0$.

current. Therefore, a positively (negatively) charged particle has positive (negative) convective and concentration gradient surface currents. Because the bulk conductivity is always positive, this leads to $\mathrm{Du} < 0$ when $\zeta < 0$ and $\mathrm{Du} > 0$ when $\zeta > 0$ for the case of $D_+ = D_-$ with KCl.

By assuming the diffusivities are equal, we are effectively neglecting the electromigrative contribution to the surface current, $\epsilon \int_0^\infty \sum_i z_i^2 D_i (n_i^0 - n_i^\infty)\theta dy \mathbf{V}$, since $\theta = 0$. If we allowed the electric field to be nonzero, however, the electromigrative surface current would be positive (negative) for a positive (negative) value of θ, regardless of the sign of the ζ potential. In summary, a negative value for Du is possible when $\theta < 0$, or when $\theta \geqslant 0$ if $\zeta < 0$.

As with EP, we can turn to streamlines of the perturbed electrostatic potential and neutral salt concentration fields to help explain the effect of surface conduction on mobility. At large $|\mathrm{Du}|$,

$$\phi^1 = \frac{3\mathrm{sgn}(\zeta)}{4r^3}\left(\boldsymbol{\nabla} \ln N_+^\infty\right) \cdot \mathbf{r}, \tag{38a}$$

$$c^1 = n_+^1 + n_-^1 = 2\left(1 - \frac{1}{4r^3}\right)\left(\boldsymbol{\nabla} \ln N_+^\infty\right) \cdot \mathbf{r}, \tag{38b}$$

which in comparing with (36) we see the roles of ϕ^1 and c^1 are reversed from EP. This similarity is readily understood: in EP, $-\boldsymbol{\nabla}\phi^1|_{r\to\infty} = \mathbf{E}^\infty$ is the applied, uniform field and the bulk concentration gradient $-\boldsymbol{\nabla}c^1$ is a result of surface conduction. Conversely, in DP, $\boldsymbol{\nabla}c^1|_{r\to\infty}$ is the applied and uniform field and $-\boldsymbol{\nabla}\phi^1$ is the result of surface conduction. As such, the explanation for the mobility maximum is similar to that for EP. Specifically, from Fig. 4(b) we see that the concentration flux is uniform far from the sphere and varies across the surface (the interface between the thin diffuse layer and the bulk). This drives a tangentially varying surface flux of counterions (negative ions). This simultaneously directs bulk concentration field lines into (out of) the diffuse layer over the downstream (upstream) regions—relative to the applied concentration gradient. To prevent coions from entering the diffuse layer, a bulk electric field [Fig. 4(e)] is established that induces

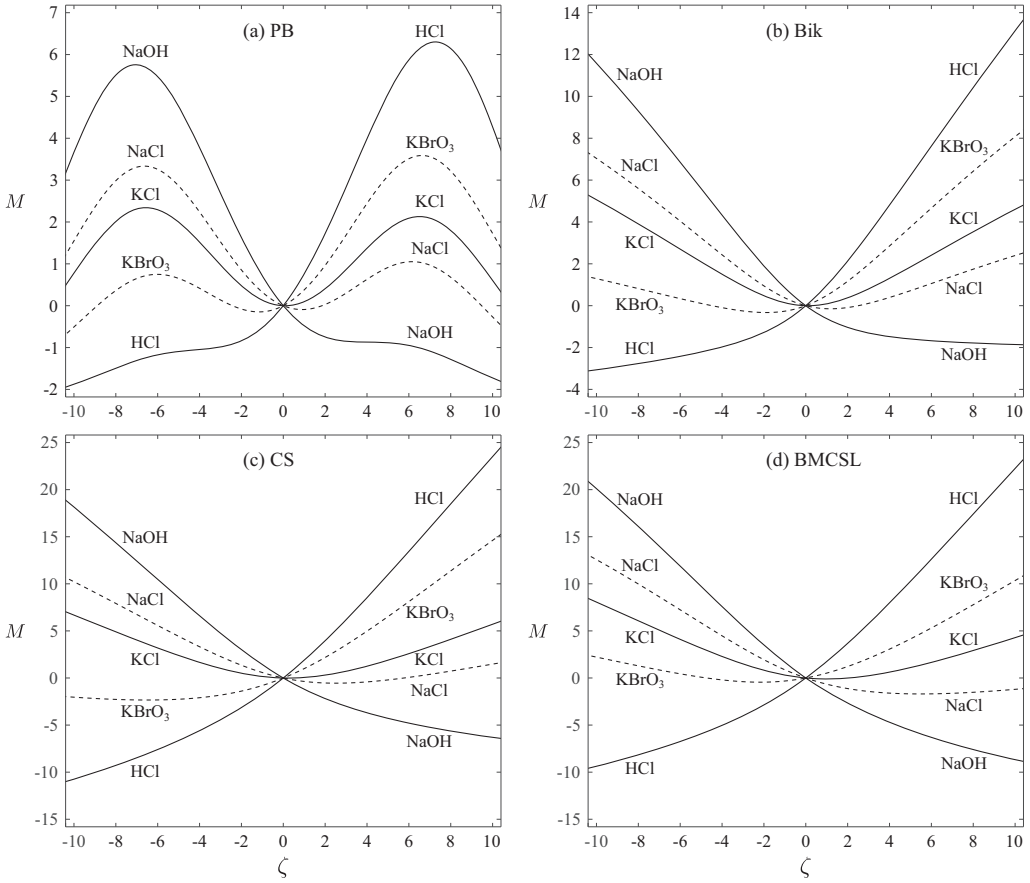

FIG. 5. Diffusiophoretic mobility vs ζ potential for different salts using (a) PNP, (b) Bik, (c) CS, and (d) BMCSL. The salts have the following values for β^{id}: NaOH (-0.5962), NaCl (-0.2074), KCl (-0.0188), KBrO3 (0.2618), and HCl (0.6417). All concentrations are 1 M and $\epsilon = 0.01$. The dashed and solid lines are to aid readability.

an electro-osmotic flow which counteracts the chemiosmotic flow, resulting in a reduced mobility. Therefore, the mobility maximum is not observed when steric repulsion is taken into account because of the reduced surface conduction arising from reduced counterion densities within the diffuse layer.

2. Asymmetric electrolytes ($D_+ \neq D_-$)

For real salts, the diffusivities are unequal and $\beta^{\mathrm{id}} \neq 0$. Figure 5 is a plot of ζ potential versus mobility for 1 M solutions of several different electrolytes using all four models. We see the expected behavior of a mobility maximum in PB and no maximum for all models of ion size due to the effect of reducing surface conduction.

For PB, Bik, and CS, as $|\beta^{\mathrm{id}}|$ increases, the asymmetry in the mobility will increase and the larger mobility will be that for which $\beta^{\mathrm{id}}\zeta > 0$. When this condition is met, the electrophoretic contribution to the mobility will be towards higher concentrations and support the chemiphoretic contribution which always acts towards higher concentrations. This generalization is possible because the ions are assumed to be the same size in these three models and $\theta = \beta^{\mathrm{id}}(1 + H)$. As for the above case of symmetric electrolytes, the BMCSL model incorporates the additional asymmetry of different sized ions and such a generalization is not possible due to the more complex dependence of the induced electric field on diffusivity and ion size [see (15c)]. However we observe the same general trend

in Fig. 5(d) and predict that the larger mobility will be for that colloid and electrolyte for which $\theta\zeta > 0$.

For nonzero β^{id}, the equations for the perturbed electrostatic potential and neutral salt density in the bulk for the PB model at large |Du| are

$$\phi^1 = \left[-\beta^{\mathrm{id}}\left(1 - \frac{1}{4r^3}\right) + \frac{3\mathrm{sgn}(\zeta)}{4r^3}\right](\nabla \ln N^\infty)\cdot \mathbf{r}, \tag{39a}$$

$$c^1 = 2\left[\left(1 - \frac{1}{4r^3}\right) - \frac{3\mathrm{sgn}(\zeta)}{4r^3}\beta^{\mathrm{id}}\right](\nabla \ln N^\infty)\cdot \mathbf{r}. \tag{39b}$$

The terms containing β^{id} are the electrophoretic contribution and setting $\beta^{\mathrm{id}} = 0$ recovers the results in (38).

The effect of β^{id} on the streamlines is shown in Fig. 4 for $\zeta > 0$. For all possible values of β^{id} ($-1 < \beta^{\mathrm{id}} < 1$), a "local" electric field is generated by the same surface conduction mechanism described above for symmetric electrolytes, i.e., $\beta^{\mathrm{id}} = 0$. This electric field is directed outward over the downstream region and inward over the upstream region of the sphere (relative to the concentration gradient). Because of this, the induced electric field (far from the sphere) for $\beta^{\mathrm{id}} < 0$ cannot participate in the exchange of countercharge between the diffuse layer and the bulk solution. However, for $\beta^{\mathrm{id}} > 0$, it can serve as a source of field lines for the exchange of countercharge. As β^{id} becomes more positive, the concentration flux lines are directed more normal to the surface. This leads to a decrease in the magnitude of the tangential flux and hence a reduced mobility (for a positively charged surface, where $\zeta \to +\infty$). Note that this is not shown in Fig. 5(a) as the large ζ behavior does not become apparent for the electrolytes given until $|\zeta| \approx 15$, which is not experimentally feasible.

To directly compare EP to DP in the limit of large ζ for PB, we can simplify Eq. (29) for the limit of large ζ with ϵ fixed (i.e., $|\mathrm{Du}| \to \infty$) and for $z_+ = -z_- = z$. In this limit, the mobility equation simplifies to

$$M = \begin{cases} \frac{\mathrm{sgn}(\zeta)}{z}\ln 4, & \text{for EP,} \\ (\mathrm{sgn}(\zeta) z\beta^{\mathrm{id}} - 1)\frac{1}{z^2}\ln 4, & \text{for DP.} \end{cases} \tag{40}$$

The result in (40) for EP is known [35,36,48]. In both EP and DP, the mobility becomes independent of $|\zeta|$, depending only the sign of the ζ potential. From (40), we see that the EP mobility has the same sign as the ζ potential, indicating that positively (negatively) charged particles move with (against) the electric field. However, for DP, it is straightforward to show that the mobility is negative (i.e., toward lower concentrations) for any electrolyte and particle ζ potential since $|\beta^{\mathrm{id}}| < 1/z$. This indicates that large surface conduction effects, such as the local electric field, dominate the diffusiophoretic motion of the particle in the limit of large ζ. Again, these limiting values are approached when $|\zeta| \gtrsim 15$ and thus not observed in Fig. 5.

V. PHORETIC MOBILITY: FOR VARYING CONCENTRATION AT FIXED SURFACE CHARGE DENSITY

Here, we consider a colloid with a constant, uniform surface charge density and vary the concentration of the electrolyte solution (i.e., ϵ). This is a more relevant point of view to how experiments involving electrophoresis and diffusiophoresis are typically carried out. That is, it is difficult to vary the ζ potential while keeping the Debye layer thickness fixed (as both are functions of concentration), as was the focus of the previous section. If the electrolyte consists of potential determining ions, changing the electrolyte concentration can ionize or deionize chemically active sites on the particle surface such that both the ζ potential and surface charge density change with concentration [49]. Here, we assume a constant surface charge density and thus do not account for this effect.

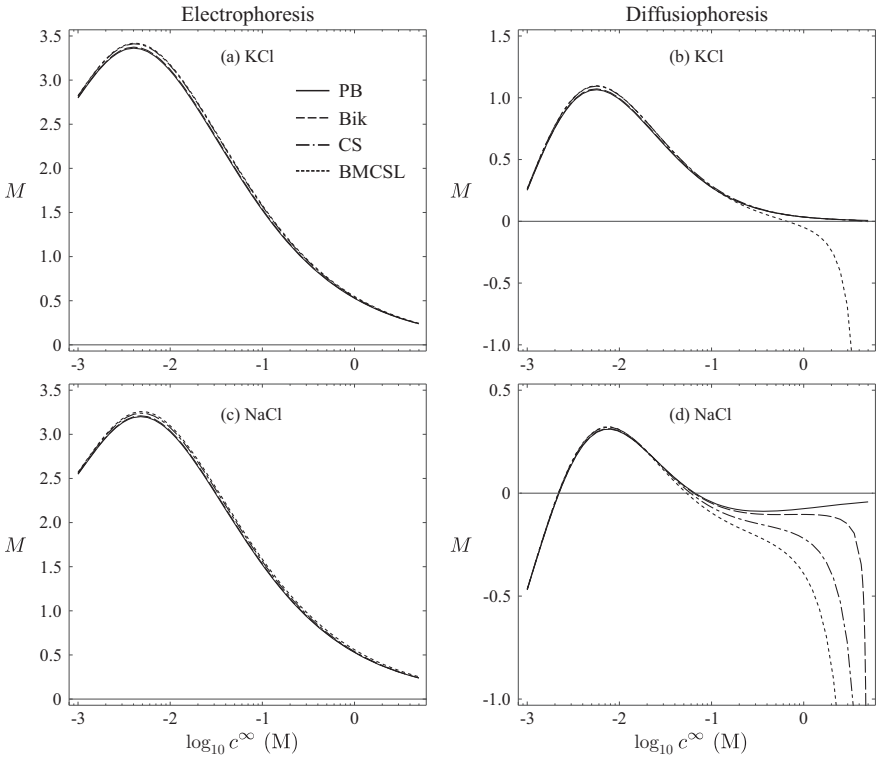

FIG. 6. The phoretic mobility for a colloid with constant surface charge density $\Gamma^* = 3\ \mu\text{C/cm}^2$ in a solution of KCl (where $D_+ = D_-$) (a),(b) and NaCl (c),(d). The electrophoretic mobility (a),(c) shows essentially no difference between the four models while the diffusiophoretic mobility (b),(d) has significant variation at large concentrations due to the rapidly increasing induced electric field. The BMCSL model deviates in KCl (b) because it retains a nonzero β^{ex} when $D_+ = D_-$.

We denote the dimensional surface charge density as Γ^* and use Gauss's law to relate it to the electrostatic potential at the surface, $-\varepsilon\hat{\mathbf{n}} \cdot \boldsymbol{\nabla}\phi = \Gamma^*$ [1]. In terms of the local planar coordinate, y, we replace boundary condition (22a) with

$$\left.\frac{d\phi}{dy}\right|_{y=0} = -\epsilon\Gamma, \tag{41}$$

where $\Gamma = \Gamma^*/(\varepsilon k_B T/eR)$ is the dimensionless surface charge density. For the purposes of calculating ϵ, we assumed a colloid radius of $R = 210$ nm. For PB, it is straightforward to derive Graham's equation, $\Gamma = 2\sqrt{2}\epsilon \sinh(z\zeta/2)$, for $z_+ = -z_- = z$, which relates the ζ potential, surface charge density, and bulk concentration [1]. It is generally not possible to derive analogous closed-form equations for ion steric models except for Bik [22].

Figure 6 plots electrophoretic mobility and diffusiophoretic mobility versus concentration (up to a maximum concentration of 5 M) for a spherical colloid with a uniform surface charge density of 3.0 $\mu\text{C/cm}^2$. This value for surface charge density is used as an intermediate value in the range typically encountered [50,51]. For the concentration range shown, $1\ \text{mM} \leqslant c^{\infty} \leqslant 5\ \text{M}$, the diffuse layer is still quite thin, $0.062 \leqslant \epsilon \leqslant 8.77 \times 10^{-4}$, even with the particle size of $R = 210$ nm. Figures 6(a) and 6(b) are for the symmetric treatment of KCl for which we assume the diffusivities are equal ($\beta^{\text{id}} = 0$); Figs. 6(c) and 6(d) are for the asymmetric case of NaCl. We see that the electrophoretic mobility is essentially the same in both electrolytes for all four models; indicating

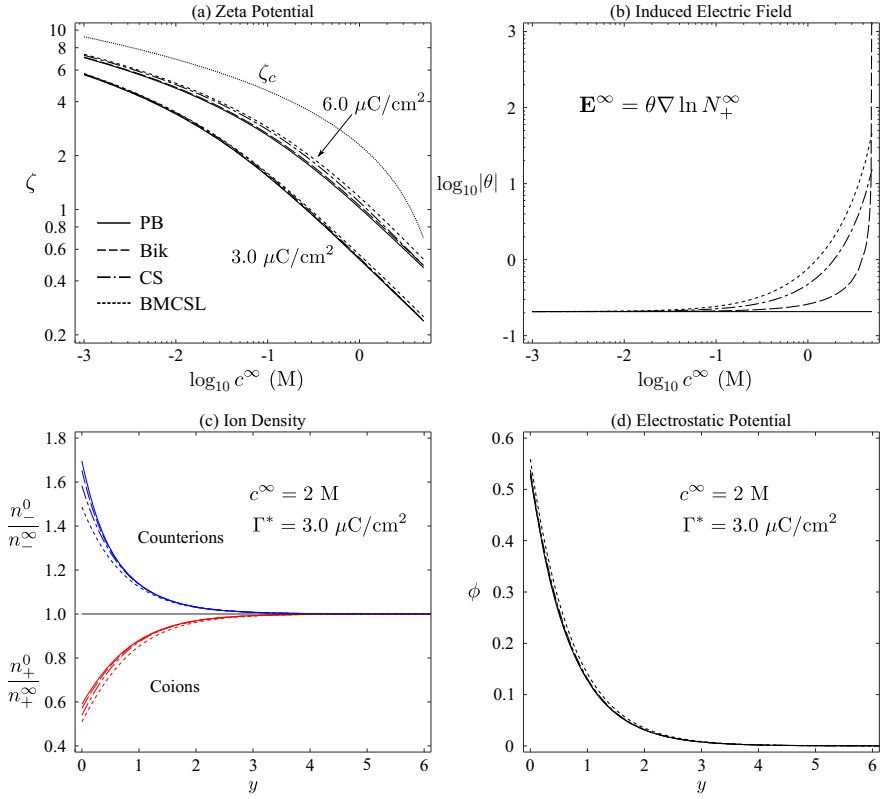

FIG. 7. A colloid of constant surface charge density in a solution of NaCl. The ζ potential (a) calculated using the four models for surface charge densities of $\Gamma^* = 3$ and 6 μC/cm^2. Also shown is the critical ζ potential, ζ_c; above which ion steric effects are expected to be important. Despite slight deviation from the classic PB model result for 6 μC/cm^2, all models predict ζ potentials below the critical value. The induced electric field (b) increases with increasing concentration in all models except the PB model which does not account for ion size. The rate at which the electric field increases is greater than the rate at which the ζ potential decreases. Panels (c) and (d) are for $\Gamma^* = 3$ μC/cm^2 and $c^\infty = 2$ M. All four models predict essentially the same structure of the diffuse layer in terms of both the equilibrium ion densities (c) and the electrostatic potential (d) despite the large concentration.

that, surprisingly, there is no appreciable difference in the predictions between the simple PB model and the more complex models for ion size.

We see that in KCl, the diffusiophoretic mobility predicted from PB, Bik, and CS are essentially the same as well; BMCSL differs only at large concentrations. In NaCl, all three models incorporating ion size predict qualitatively different diffusiophoretic mobilities compared with the PB model.

This large concentration behavior can be understood in terms of the ζ potential and induced electric field. Figure 7(a) is a plot of ζ potential versus concentration in NaCl. All four models predict that the ζ potential decreases with increasing electrolyte concentration, and all three models for ion size predict values of ζ that are in good agreement with that predicted by the simple PB model. In addition, since the ζ potential for all models is below the critical ζ potential ζ_c, at which ion sterics are expected to be important, this has the consequence of rendering ion steric effects negligible within the diffuse layer. Therefore, when the bulk concentration is large, the ζ potential is small and the total ion density in the diffuse layer is not much greater than in the bulk. This is seen in Figs. 7(c) and 7(d) which show that the structure of the equilibrium diffuse layer does not vary appreciably between the four models despite the rather large concentration of 1 M, where $\Phi^\infty = 0.201$, 0.105,

and 0.110, for Bik, CS, and BMCSL, respectively. In addition, the equilibrium ion densities in Fig. 7(c) are on the order of the bulk concentration and the phoretic mobility (29) and (33) only depends on the diffuse layer ion density relative to the bulk. Since EP depends only on the structure of the equilibrium diffuse layer, steric repulsion (ion size effects) does not effect electrophoretic mobility in this experimentally relevant scenario. Further, note that since the ζ potential decreases with increasing concentration, the EP mobility approaches zero at large concentrations.

However, Fig. 7(b) is a plot of the induced electric field versus concentration from DP. While the PB model predicts a constant value, the three models which account for the size of the ions predict an increasing electric field with increasing concentration. Physically, this is due to the steric repulsion between the ions as they diffuse down the concentration gradient, which as we showed in Sec. III(a), enhances the induced electric field.

Importantly, when $\zeta = 0$, there is no interaction potential between the colloid and the ions, and there will be no phoretic mobility (see Fig. 5). However, since $\zeta \propto \ln(1/\sqrt{c^\infty})$, there will always be a finite ζ potential since an electrolyte concentration has finite physical limits. In addition, while the ζ potential, and hence the interaction potential, is a slowly decreasing logarithmic function of concentration, the induced electric field (via H_i^∞) is a rapidly increasing function of concentration. For example, from (6) and (12), $\mathbf{E}^\infty \propto 1/(1-\Phi^\infty)^4$ for the CS model; recall that $\Phi^\infty \propto c^\infty$. Since the induced electric field increases more rapidly than the ζ potential decreases, the diffusiophoretic mobility is not only nonzero at large concentration but actually increases [Fig. 6(d)].

For both Figs. 6 and 7, the Bik model only goes up to a concentration of 4.03 M for KCl and 4.96 M for NaCl. This is due to assuming the ions take up a cubic volume and hence have a larger volume fraction than the CS and BMCSL models, which use ions with a spherical volume. For example, at $c^\infty = 5$ M for NaCl, the theoretical bulk volume fraction predicted by Bik is 1.007 while CS and BMCSL predict the bulk volume fraction to be 0.527 and 0.552, respectively.

VI. CONCLUSION

We have derived a general equation for the diffusiophoretic and electrophoretic mobility of a single colloid in a binary electrolyte. To describe the electrolyte, we have utilized three different models which incorporate steric repulsion between finite sized ions into the governing equations, in addition to the classic Poisson-Boltzmann model for pointlike, noninteracting ions. We show that the maximums in the mobility (with increasing ζ potential) for both diffusiophoresis and electrophoresis that are predicted by the Poisson-Boltzmann model are essentially eliminated by accounting for ion size. This is readily understood: the effect of ion sterics on the equilibrium diffuse layer is to reduce the counterion density relative to the Poisson-Boltzmann model. Since the maximum in mobility is due to a rapidly increasing surface conduction, the reduced counterion density reduces the surface conduction and an opposing chemiosmotic (in electrophoresis) or electro-osmotic (in diffusiophoresis) flow does not develop. The mobility therefore does not undergo a maximum over realistic values for the ζ potential.

For a colloid with a constant surface charge density, a more relevant scenario for experiments, we show that, surprisingly, ion size effects are much more important for diffusiophoresis at high concentrations than for electrophoresis. This is because as the ζ potential decreases (and hence counterion density, relative to the bulk, decreases) with increasing concentration, steric repulsion between ions does not affect the structure of the diffuse layer for reasonable surface charge densities. However, steric repulsion within the highly concentrated bulk solution is non-negligible. Therefore, when there is an applied concentration gradient, as in diffusiophoresis (not electrophoresis), there exists an additional effect due to the size of the ions: a gradient in the excess electrochemical potential, which leads to an increase in the induced electric field with increasing concentration. Electrophoresis has no concentration gradient in the bulk solution and therefore has no excess electrochemical potential gradient. Therefore, since steric repulsion minimally affects the diffuse layer structure, the electrophoretic mobility is minimally affected by ion size effects (for ζ potentials resulting from a reasonable constant surface charge density).

Our predictions for diffusiophoresis are contrary to the common notion that the phoretic mobility approaches zero with increasing concentration due to a decreasing ζ potential [1]. While this notion holds for electrophoresis, for diffusiophoresis, it is only predicted by the Poisson-Boltzmann model. For any real electrolyte, for which the diffusivities are not equal, any model that includes steric repulsion between ions will predict an increase in the diffusiophoretic mobility with increasing concentration [see Fig. 6(d)]. Hence, far from becoming immobile, we predict that the mobility will actually increase greatly in concentrated electrolytes. Thus it may be that diffusiophoresis is an attractive transport mechanism in high salinity environments. Despite this increasing mobility with a decreasing ζ potential, when the ζ potential is exactly zero, the mobility is also zero (see Fig. 5). This is because there would no longer be an excess of ions surrounding the particle and therefore no slip velocity [see Eq. (26)].

Hence, the remarkable conclusion here is that to calculate the diffusiophoretic mobility of a spherical colloid, the classic Poisson-Boltzmann treatment of the electrolyte is sufficient to determine the ion profiles within the diffuse layer for reasonable surface charge densities. Then, including ion sterics within the bulk solution to derive the excess contribution to the induced electric field is straightforward by using an excess electrochemical potential. All that is required is a model for the the excess electrochemical potential and $\partial \mu_i^{\mathrm{ex}}/\partial \Phi$ evaluated at the electroneutral solution concentration. These derivatives are provided in the Appendix for the three models we considered.

In all of our results for diffusiophoresis, there is considerable dependence on which model is used to predict the mobility. This is simply due to the differences between how the models describe the ions. The Bikerman model assumes the ions occupy a regular lattice. The Carnahan-Starling and Boublik-Mansoori-Carnahan-Starling-Leland models are based on liquid-state theory for hard spheres, the latter being for a general case of different sized spheres while the former is for the special case of spheres of the same size. Our work in this paper uses equations which are valid under the local density approximation (LDA). The equilibrium profiles calculated under this assumption are not always as accurate at high concentrations as methods based on density functional theory (DFT) or molecular simulations. However, these equilibrium profiles are only an intermediate step towards calculating the mobility. Such integrated quantities (including capacitance) have been shown to agree well with DFT and molecular simulations [31,32]. However, by using a fourth order Poisson equation which accounts for electrostatic correlations between ions, it has been shown that the equilibrium profiles can achieve better agreement with those from simulations, including local oscillations of charge density due to overscreening [52,53]. This "modified-Poisson equation" has also been shown to predict electrophoretic mobility reversals in agreement with experiments in concentrated, multivalent electrolytes [54]. Incorporation of ion electrostatic correlation effects into diffusiophoresis is left for future work. Other effects in concentrated electrolytes include variations in the viscosity and permittivity [22]. As the electrolyte concentration increases, it is expected that the viscosity will also increase and the permittivity will decrease. Given this, it is possible that including these effects could reduce the large increase in diffusiophoretic mobility that we predict.

It should be noted that although our final equation for mobility (29) is independent of which model for the excess electrochemical potential is chosen to describe the electrolyte, it needs to be expressible as a function of the local (or bulk) volume fraction of ions only [i.e., $\mu_i^{\mathrm{ex}} = \mu_i^{\mathrm{ex}}(\Phi)$]. As we show in the derivation, this is required to express $\boldsymbol{\nabla} \mu_i^{\mathrm{ex}}$ in terms of the applied gradient, $\boldsymbol{\nabla} \ln N_+^{\infty}$. A consequence of this is that even though certain models used in DFT can be expressed as excess electrochemical potentials [31], they cannot be used in conjunction with our final Eq. (29). However, substitution of *any* excess electrochemical potential model into (11) is still possible, but derivation of a single final equation for the phoretic mobility—as we have done—would not readily follow.

Although we have considered the separate application of a concentration gradient and an electric field, the simultaneous action of both is a common situation in electrochemical cells and termed "electrodiffusiophoresis" [55]. In such situations, reversals in particle migration direction can be brought about by altering the applied electrical current in addition to an appropriate selection of electrolyte and gradient strength [55]. When both an electric field and concentration gradient are applied, the electrophoretic and diffusiophoretic contributions to particle motion combine nonlinearly

and the particle migration velocity increases in lower concentration regions due to an increase in the electric field in these regions. An interesting question then is whether ion sterics will increase the electric field in the high concentration region (as we predict) relative to the low concentration regions in electrodiffusiophoresis.

ACKNOWLEDGMENTS

We acknowledge support from NSF CAREER Award No. CBET-1350647.

APPENDIX

1. Solution method for the equilibrium diffuse layer and excess electrochemical potential derivatives

To obtain the equilibrium profiles of ion density and electrostatic potential, we used MATLAB and a finite differencing scheme to solve Poisson's equation subject to the algebraic equations generated by the constraint of a constant electrochemical potential. In general, these equations are

$$\frac{d^2\phi}{dy^2} + (z_+ n_+ + z_- n_-) = 0, \tag{A1a}$$

$$z_i\phi + \ln n_i - \ln n_i^\infty + \mu_i^{\mathrm{ex}} - \mu_i^{\mathrm{ex},\infty} = 0, \tag{A1b}$$

in terms of the local planar coordinate, $y = (r-1)/\epsilon$ and where $i = +$ and $i = -$ for the cation and anion species, respectively. For the case of a specified ζ potential, we first use (A1b) to obtain the ion densities at the surface, then apply both Eqs. (A1a) and (A1b) to the remainder of the problem domain. Since both ϕ and n_i decay to a constant as $y \to \infty$, it is only necessary to include a finite distance. We used a domain of $y = [0,20]$, which we tested and found $y = 20$ to be sufficiently far from the surface that increases do not affect the results presented in the main text.

Once the equilibrium profiles are known, it is straightforward to evaluate the requisite integrals to obtain the mobility. However, it is useful to include the expressions for the excess electrochemical potential gradients H_i^∞ for the three models we used, especially considering this is essentially all that is necessary to predict the effects of ion size on diffusiophoresis. Recall that $H_i^\infty = \Phi^\infty \partial\mu_i^{\mathrm{ex}}/\partial\Phi^\infty$, where $\Phi^\infty = \sum_i N_i^\infty v_i$ is the volume fraction of ions in the bulk solution and N_i^∞ is the number density of ion species i.

The expressions for the excess electrochemical potential can be found in the text (5)–(7). The expressions for H_i^∞ are

$$H_i^\infty = \begin{cases} \frac{\Phi^\infty}{1-\Phi^\infty}, & \text{for Bik,} \\ \frac{2\Phi^\infty(4-\Phi^\infty)}{(1-\Phi^\infty)^4}, & \text{for CS,} \\ (T_{i,1}+T_{i,2}+T_{i,3}+T_{i,4})\frac{1}{(\Phi^\infty)^2(1-\Phi^\infty)^4}, & \text{for BMCSL,} \end{cases} \tag{A2a}$$

where

$$T_{i,1} = \left[1 + 2\left(\frac{\xi_2^\infty a_i}{\Phi^\infty}\right)^3 - 3\left(\frac{\xi_2^\infty a_i}{\Phi^\infty}\right)^2\right](\Phi^\infty(1-\Phi^\infty))^3, \tag{A3a}$$

$$T_{i,2} = \left(3\xi_2^\infty a_i + 3\xi_1^\infty a_i^2 + \xi_0^\infty a_i^3\right)(\Phi^\infty(1-\Phi^\infty))^2, \tag{A3b}$$

$$T_{i,3} = 3\xi_2^\infty a_i^2\left[\xi_2^\infty(1+\Phi^\infty) + 2\Phi^\infty\xi_1^\infty a_i\right]\Phi^\infty(1-\Phi^\infty), \tag{A3c}$$

$$T_{i,4} = -2\left(\xi_2^\infty\right)^3 a_i^3[1 - 3\Phi^\infty - (\Phi^\infty)^2], \tag{A3d}$$

and $\xi_k^\infty = \sum_j N_j^\infty v_j a_j^{k-3}$.

2. Streamline equations for a general binary electrolyte

Here, we provide the equations for the perturbed electrostatic potential and salt concentration for the PB model for a general binary electrolyte. By taking appropriate linear combinations of the perturbed electrochemical potentials, we obtain

$$\phi^1 = \frac{\mu_+^1 - \mu_-^1}{z_+ - z_-}, \tag{A4a}$$

$$c^1 = \frac{2(z_-\mu_+^1 - z_+\mu_-^1)}{z_+z_-(z_+ - z_-)}. \tag{A4b}$$

Substituting (27) for μ_i^1 and (17b) for the definition of G_i, we obtain

$$\phi^1 = \begin{cases} \left[-1 + \frac{\Delta_\phi C}{(z_+-z_-)r^3}\right]\mathbf{V}\cdot\mathbf{r}, & \text{for EP,} \\ \left[-\beta^{\mathrm{id}} + \frac{\Delta_\phi C}{(z_+-z_-)r^3}\right]\mathbf{V}\cdot\mathbf{r}, & \text{for DP,} \end{cases} \tag{A5a}$$

$$c^1 = \begin{cases} \frac{2\Delta_c C}{z_+(z_+-z_-)r^3}\mathbf{V}\cdot\mathbf{r}, & \text{for EP,} \\ 2\left[-\frac{1}{z_+z_-} + \frac{\Delta_c C}{z_+(z_+-z_-)r^3}\right]\mathbf{V}\cdot\mathbf{r}, & \text{for DP,} \end{cases} \tag{A5b}$$

for any ζ, where $\Delta_\phi C = C_+ - C_-$ and $\Delta_c C = C_+ - z_+C_-/z_-$ and C_i are given by (32). For large ζ with ϵ fixed (or equivalently, large Du), coions (co) are excluded from the diffuse layer so $\partial\mu_{\mathrm{co}}/\partial r|_{r=1} = 0$ and the diffuse layer acts as a conductor of counterions (cnt) with $\nabla_s\mu_{\mathrm{cnt}}|_{r=1} = 0$. This gives $C_{\mathrm{co}} = G_{\mathrm{co}}/2$ and $C_{\mathrm{cnt}} = -G_{\mathrm{cnt}}$ from (32). Substituting this into the above we obtain

$$\phi^1 = \begin{cases} -\beta^{\mathrm{id}}\left(1 + \frac{z_{\mathrm{co}}+2z_{\mathrm{cnt}}}{2(z_+-z_-)r^3}\mathrm{sgn}(\zeta)\right)\mathbf{V}\cdot\mathbf{r}, & \text{for EP,} \\ \left[-\beta^{\mathrm{id}}\left(1 + \frac{z_{\mathrm{co}}+2z_{\mathrm{cnt}}}{2(z_+-z_-)r^3}\mathrm{sgn}(\zeta)\right) + \frac{3\mathrm{sgn}(\zeta)}{2(z_+-z_-)r^3}\right]\mathbf{V}\cdot\mathbf{r}, & \text{for DP,} \end{cases} \tag{A6a}$$

$$c^1 = \begin{cases} -\frac{3\mathrm{sgn}(\zeta)}{(z_+-z_-)r^3}\beta^{\mathrm{id}}\mathbf{V}\cdot\mathbf{r}, & \text{for EP,} \\ 2\left[-\frac{1}{z_+z_-}\left(1 - \frac{2z_{\mathrm{co}}+z_{\mathrm{cnt}}}{2(z_+-z_-)r^3}\mathrm{sgn}(\zeta)\right) - \frac{3\mathrm{sgn}(\zeta)}{2(z_+-z_-)r^3}\beta^{\mathrm{id}}\right]\mathbf{V}\cdot\mathbf{r}, & \text{for DP.} \end{cases} \tag{A6b}$$

For $z_+ = 1$ and $z_- = -1$, we obtain Eqs. (36), (38), and (39).

[1] W. B. Russel, D. A. Saville, and W. R. Schowalter, *Colloidal Dispersions* (Cambridge University Press, Cambridge, England, 1989).

[2] D. C. Prieve, J. L. Anderson, J. P. Ebel, and M. E. Lowell, Motion of a particle generated by chemical gradients. Part 2. Electrolytes, J. Fluid Mech. **148**, 247 (1984).

[3] J. L. Anderson, M. E. Lowell, and D. C. Prieve, Motion of a particle generated by chemical gradients. Part 1. Non-electrolytes, J. Fluid Mech. **117**, 107 (1982).

[4] J. S. Paustian, C. D. Angulo, R. Nery-Azevedo, N. Shi, A. I. Abdel-Fattah, and T. M. Squires, Direct measurements of colloidal solvophoresis under imposed solvent and solute gradients, Langmuir **31**, 4402 (2015).

[5] B. V. Derjaguin, G. P. Sidorenkov, E. A. Zubashchenkov, and E. V. Kiseleva, Kinetic phenomena in boundary films of liquids, Kolloidn. Zh. **9**, 335 (1947).

[6] J. L. Anderson and D. C. Prieve, Diffusiophoresis caused by gradients of strongly adsorbing solutes, Langmuir **7**, 403 (1991).

[7] N. Sharifi-Mood, J. Koplik, and C. Maldarelli, Molecular Dynamics Simulation of the Motion of Colloidal Nanoparticles in a Solute Concentration Gradient and a Comparison to the Continuum Limit, Phys. Rev. Lett. **111**, 184501 (2013).

[8] N. Sharifi-Mood, J. Koplik, and C. Maldarelli, Diffusiophoretic self-propulsion of colloids driven by a surface reaction: The sub-micron particle regime for exponential and van der Waals interactions, Phys. Fluids. **25**, 012001 (2013).
[9] M. von Smoluchowski, Contribution à la théorie de l'endosmose électrique et de quelques phenomènes corrélatifs, Bull. Int. Acad. Sci. Cracovie **8**, 182 (1903).
[10] T. M. Squires and S. R. Quake, Microfluidics: Fluid physics at the nanoliter scale, Rev. Mod. Phys. **77**, 977 (2005).
[11] K. D. Dorfman, DNA electrophoresis in microfabricated devices, Rev. Mod. Phys. **82**, 2903 (2010).
[12] A. A. Elbashir and H. Y. Aboul-Enein, Capillary electrophoresis and molecular modeling as a complementary technique for chiral recognition mechanism, Crit. Rev. Anal. Chem. **43**, 131 (2013).
[13] R. Guha, X. Shang, A. L. Zydney, D. Velegol, and M. Kumar, Diffusiophoresis contributes significantly to colloidal fouling in low salinity reverse osmosis systems, J. Membrane Sci. **479**, 67 (2015).
[14] A. Kar, R. Guha, N. Dani, D. Velegol, and M. Kumar, Particle deposition on microporous membranes can be enhanced or reduced by salt gradients, Langmuir **30**, 793 (2014).
[15] A. Kar, T. Chiang, I. O. Rivera, A. Sen, and D. Velegol, Enhanced transport into and out of dead-end pores, ACS Nano **9**, 746 (2015).
[16] B. Abécassis, C. Cottin-Bizonne, C. Ybert, A. Ajdari, and L. Bocquet, Boosting migration of large particles by solute contrasts, Nat. Mater. **7**, 785 (2008).
[17] V. Yadav, J. D. Freedman, M. Grinstaff, and A. Sen, Bone-crack detection, targeting, and repair using ion gradients, Angew. Chem.- Int. Ed. **52**, 10997 (2013).
[18] V. Yadav, R. A. Pavlick, S. M. Meckler, and A. Sen, Triggered detection and deposition: Toward the repair of microcracks, Chem. Mater. **26**, 4647 (2014).
[19] D. Velegol, A. Garg, R. Guha, A. Kar, and M. Kumar, Origins of concentration gradients for diffusiophoresis, Soft Matter. **12**, 4686 (2016).
[20] M. S. Kilic, M. Z. Bazant, and A. Ajdari, Steric effects in the dynamics of electrolytes at large applied voltages, I. Double-layer charging, Phys. Rev. E. **75**, 021502 (2007).
[21] H. Ohtaki and T. Radnai, Structure and dynamics of hydrated ions, Chem. Rev. **93**, 1157 (1993).
[22] M. Z. Bazant, M. S. Kilic, B. D. Storey, and A. Ajdari, Towards an understanding of induced-charge electrokinetics at large applied voltages in concentrated solutions, Adv. Colloid Interface Sci. **152**, 48 (2009).
[23] H. G. Bagaria, Z. Xue, B. M. Neilson, A. J. Worthen, K. Y. Yoon, S. Nayak, V. Cheng, J. H. Lee, C. W. Bielawski, and K. P. Johnston, Iron oxide nanoparticles grafted with sulfonated copolymers are stable in concentrated brine at elevated temperatures and weakly adsorb on silica, ACS Appl. Mater. Interfaces **5**, 3329 (2013).
[24] A. Lager, K. J. Webb, I. R. Collins, and D. M. Richmond, *LoSal Enhanced Oil Recovery: Evidence of Enhanced Oil Recovery at the Reservoir Scale, SPE Symposium on Improved Oil Recovery, Tulsa, OK* (Society of Petroleum Engineers, Richardson, Texas, 2008).
[25] B. E. Logan and M. Elimelech, Membrane-based processes for sustainable power generation using water, Nature (London) **488**, 313 (2012).
[26] A. S. Khair and T. M. Squires, Ion steric effects on electrophoresis of a colloidal particle, J. Fluid Mech. **640**, 343 (2009).
[27] P. M. Biesheuvel and M. van Soestbergen, Counterion volume effects in mixed electrical double layers, J. Colloid Interface Sci. **316**, 490 (2007).
[28] M. Manciu and E. Ruckenstein, Lattice site exclusion effect on the double layer interaction, Langmuir **18**, 5178 (2002).
[29] J. J. Bikerman, XXXIX. Structure and capacity of electrical double layer, Philos. Mag. **33**, 384 (1942).
[30] N. F. Carnahan and K. E. Starling, Equation of state for nonattracting rigid spheres, J. Chem. Phys. **51**, 635 (1969).
[31] D. Gillespie, A review of steric interactions of ions: Why some theories succeed and others fail to account for ion size, Microfluid Nanofluid **18**, 717 (2015).

[32] B. Giera, N. Henson, E. M. Kober, M. S. Shell, and T. M. Squires, Electric double-layer structure in primitive model electrolytes: Comparing molecular dynamics with local-density approximations, Langmuir **31**, 3553 (2015).
[33] R. W. O'Brien and L. R. White, Electrophoretic mobility of a spherical colloidal particle, J. Chem. Soc. Faraday Trans. **74**, 1607 (1978).
[34] S. S. Dukhin and B. V. Deryaguin, in *Encylcopedia of Surface and Colloid Science* (Wiley, New York, 1974), Vol. 7.
[35] R. W. O'Brien, The solution of the electrokinetic equations for colloidal particles with thin double layers, J. Colloid Interface Sci. **92**, 204 (1983).
[36] A. S. Khair and T. M. Squires, The influence of hydrodynamic slip on the electrophoretic mobility of a spherical colloidal particle, Phys. Fluids. **21**, 042001 (2009).
[37] T. Boublik, Hard-sphere equation of state, J. Chem. Phys. **53**, 471 (1970).
[38] G. A. Mansoori, N. F. Carnahan, K. E. Starling, and T. W. Leland, Equilibrium thermodynamic properties of the mixture of hard spheres, J. Chem. Phys. **54**, 1523 (1971).
[39] M. M. J. Lin and D. C. Prieve, Electromigration of latex induced by a salt gradient, J. Colloid Interface Sci. **95**, 327 (1983).
[40] J. Newman and K. E. Thomas-Alyea, *Electrochemical Systems* (Wiley, New York, 2004).
[41] T. Chiang and D. Velegol, Multi-ion diffusiophoresis, J. Colloid Interface Sci. **424**, 120 (2014).
[42] O. Schnitzer and E. Yariv, Strong-field electrophoresis, J. Fluid Mech. **701**, 333 (2012).
[43] E. Yariv, An asymptotic derivation of the thin-debye-layer limit for electrokinetic phenomena, Chem. Eng. Commun. **197**, 3 (2009).
[44] J. L. Anderson, Colloid transport by interfacial forces, Annu. Rev. Fluid Mech. **21**, 61 (1989).
[45] M. Flury and T. F. Gimmi, Solute diffusion, in *Methods of Soil Analysis, Part 4, Physical Methods*, edited by J. H. Dane and G. C. Topp (Soil Science Society of America, Madison, WI, 2002), p. 1323.
[46] T. R. Ferguson and M. Z. Bazant, Nonequilibrium thermodynamics of porus electrodes, J. Electrochem. Soc. **159**, A1967 (2012).
[47] J. Lyklema, *Fundamentals of Interface and Colloid Science. Volume II: Solid-Liquid Interfaces* (Academic, London, England, 1995).
[48] H. Ohshima, Limiting electrophoretic mobility of a highly charged soft particle in an electrolyte solution: Solidification effect, J. Colloid Interface Sci. **349**, 641 (2010).
[49] J. C. Berg, *An Introduction to Interfaces and Colloids, The Bridge to Nanoscience* (World Scientific, Singapore, 2010).
[50] M. Kosmulski, Electric charge density of silica, alumina, and related surfaces, in *Encyclopedia of Surface and Colloid Science, Volume 3*, 2nd edition, edited by P. Somasundaran (Taylor and Francis Group, London, 2006).
[51] S.-L. Tsaur and R. M. Fitch, Preparation and properties of polystyrene model colloids: II. Effect of surface charge density on coagulation behavior, J. Colloid Interface Sci. **115**, 463 (1987).
[52] M. Z. Bazant, B. D. Storey, and A. A. Kornyshev, Double Layer in Ionic Liquids: Overscreening versus Crowding, Phys. Rev. Lett. **106**, 046102 (2011).
[53] B. D. Storey and M. Z. Bazant, Effects of electrostatic correlations on electrokinetic phenomena, Phys. Rev. E **86**, 056303 (2012).
[54] R. F. Stout and A. S. Khair, A continuum approach to predicting electrophoretic mobility reversals, J. Fluid Mech. **752**, R1 (2014).
[55] R. A. Rica and M. Z. Bazant, Electrodiffusiophoresis: Particle motion in electrolytes under direct current, Phys. Fluids. **22**, 112109 (2010).